Introductory Laboratory -- Nucleons
P373

γ–ray Spectroscopy with Ge(Li)
and
Abundance of Uranium Isotopes

Reference Materials

OHIO
UNIVERSITY

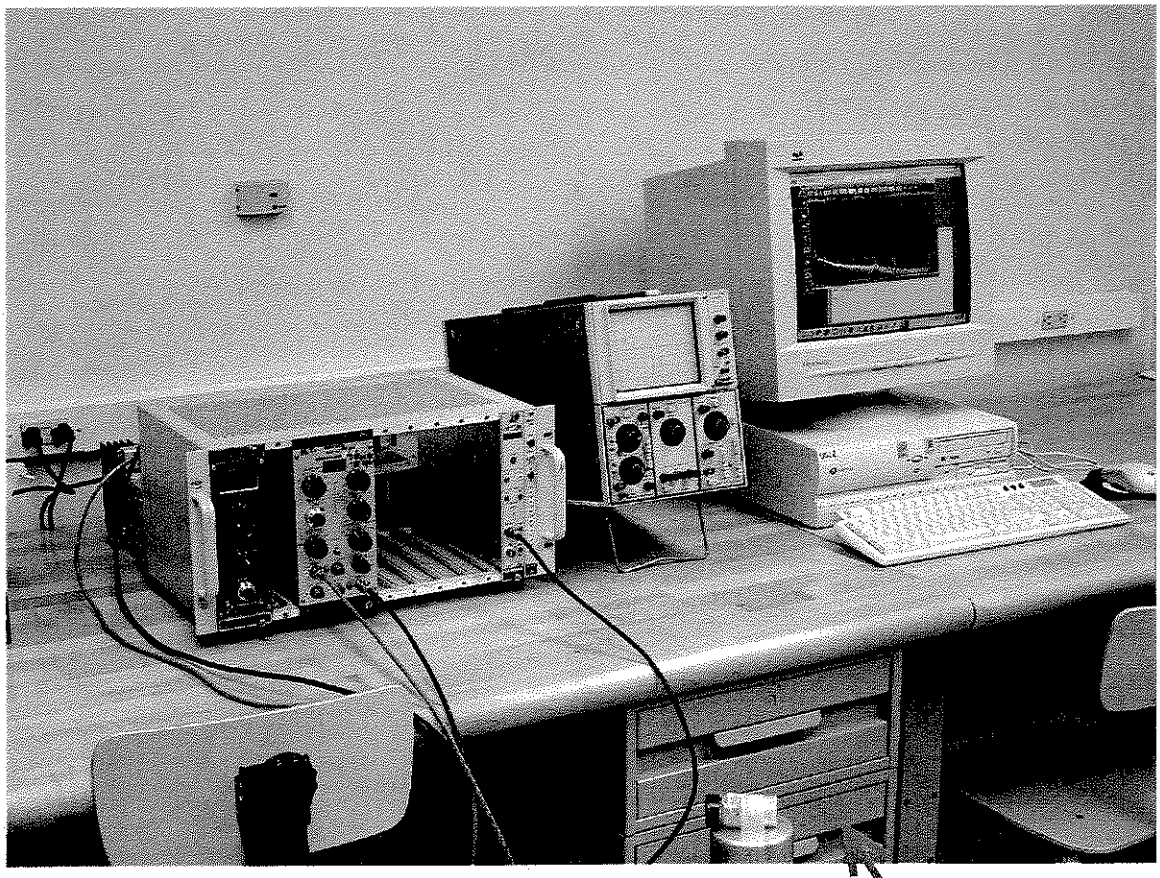

Electronics and DAQ

Ge(Li) detector + dewar

Physics 373 – Introductory Laboratory – Nucleons

γ-ray Spectroscopy with Ge(Li) and Uranium Abundances

Purpose: The purpose of this experiment is to acquaint the student with some of the basic techniques used for measuring gamma rays with high resolution, called gamma ray spectroscopy. The laboratory will also enable detailed understanding of the characteristics of the gamma ray spectrum. It is based on the use of a high purity Germanium detector drifted with Lithium HpGe(Li).

Gamma Spectroscopy: In this experiment, a HpGe detector will be used to study the gamma rays that are given off during radioactive decay of various nuclei. The detector is designed to provide excellent energy resolution, and thus it will be possible to determine with high precision the gamma ray energies present in a decay spectrum. Understanding the characteristics of the measured gamma ray spectra is an important goal of this experiment. Necessary background information for this laboratory is contained in the accompanying write-up *"Interactions of Gamma Rays with Matter"*. You may need to pursue other references as well for a complete introduction to the physics, terminology, techniques, and equipment relevant for a full understanding of this field.

List of Goals:

A). Understand the decay schemes of several different sources: ^{22}Na, ^{60}Co, ^{137}Cs, and ^{226}Ra.

B). Understand the overall electronics layout, as well as the purpose of each module employed, along with the set-up of the gates, timing, and gains.

C). Understand the detailed features of the energy spectra for each of the different sources.

D). Perform an energy calibration on the spectra using the photopeaks as reference.

E). Measure the energy resolution of the system.

F). Determine the linearity of the energy response.

G). Calibrate the energy dependence of the detector efficiency.

H). Measure the activity for ^{60}Co and ^{137}Cs sources.

I). Measure the abundance ratio of isotopes in a sample of uranium ore.

J). Keep a detailed logbook of all relevant details of this measurement.

K). Be able to access the available literature to understand the expected properties of each of the different isotopes.

L). Prepare a detailed formal lab report on all aspects of this investigation.

I. Pre-Experiment Approach and Details

◇ Before beginning the experiment, be sure to read *all* of the background material in the laboratory binder.

◇ Be sure that you have spent adequate time researching the general topic so that you can appreciate the basic ideas outlined above under the *"List of Goals"*.

◇ After performing the essential pre-lab preparations, begin to understand the experimental setup. This includes understanding the purpose of each part of the system. Get familiar with the use of the oscilloscope and how to use it to look at all of the linear signals in the setup. With no source present, why can you still see signals in the detectors? Note that manuals for each of the electronics modules used in the setup are contained in a binder in the lab room. The basic layout of the gamma ray spectroscopy system is shown in Fig. 1.

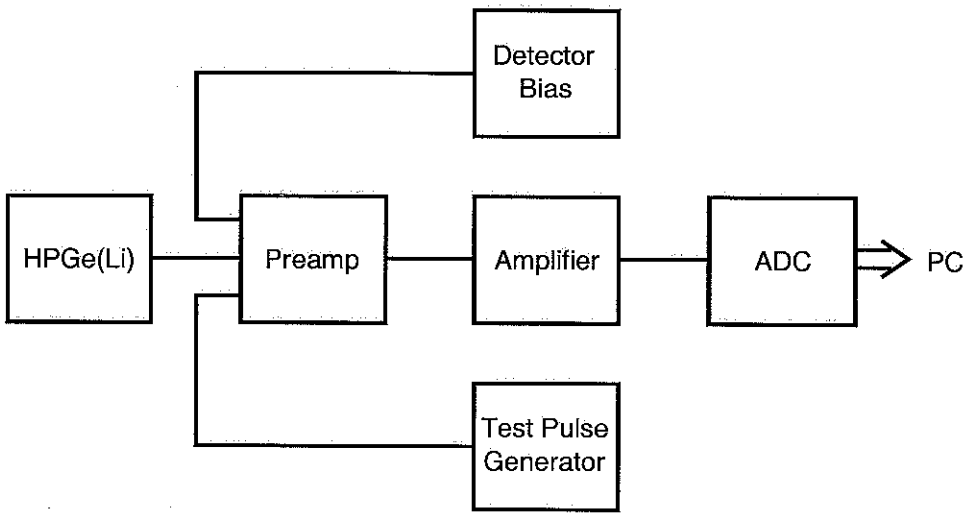

Figure 1: Major components of the gamma ray spectroscopy system set up for this laboratory.

◇ Be sure that you have full understanding of the concepts behind radiation safety and the risks inherent in using radioactive sources. Remember the adage *"time, distance, and shielding"* to minimize your exposure. Do not be afraid to ask questions. You should always strive to keep your risk of exposure as low as reasonably achievable!

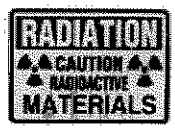

◇ After putting a source in place, go through the set-up step by step to understand how all signals look, and what the amplifier does. Be sure to provide clear and complete documentation in your logbooks. Also begin to understand how to navigate through and operate the data acquisition system.

II. Energy Resolution and Spectrum Analysis

a). Understand the qualitative features of the gamma ray spectra for the radioactive isotopes ^{22}Na and ^{137}Cs. Make sure that you can identify the relevant photopeaks, the Compton edge, and the back-scattering peak.

b). Calibrate the energy response of the Ge(Li) detector using the radioactive isotopes ^{22}Na and ^{137}Cs. This will amount to analyzing your data to produce an equation to calculate the energy of the photopeaks from the channel location information. Perform a least-squares fit to this data and list all experimental uncertainties (both statistical and systematic) that affect your measurement.

c). After your calibration has been determined, study the spectrum associated with the ^{60}Co source. Measure the energy of the photopeaks and compare to their known values.

d). Determine the energy resolution of the Ge(Li) detector using the ^{22}Na and ^{137}Cs sources. Be sure to separate the resolution intrinsic to the detector from that associated with the electronics. Compare your measured resolution with the given detector specification. Suggest any $\Delta E/E$ energy dependence your data may show.

e). Quantitatively account for the positions of the Compton edge and the back-scatter peaks in the spectra for each of the different isotopes used above.

f). Determine the linearity of the detector energy response by studying the energy calibration as a function of gamma ray energy using the National Bureau of Standards (NBS) calibrated Europium/Antimony source.

g). Understand all contributions to the NBS calibrated source spectrum. Is there evidence for any single or double escape peaks in the spectrum? Understand the dominant gamma ray interactions as a function of the gamma ray energy.

III. Efficiency of a HpGe Detector

a). Measure the peak to Compton edge amplitude ratio for the 1.33 MeV peak in ^{60}Co. Compare with the detector specification.

b). Using the NBS calibrated Eu/Sb source, compute the absolute efficiency (total absorption efficiency) of the HpGe detector as a function of gamma ray energy.

c). Using the efficiency measured from the NBS source, measure the activity of the ^{60}Co and the ^{137}Cs sources. Compare the relative activities of the two ^{60}Co photopeaks to the expectations in the literature.

IV. Uranium Isotope Abundance

Determine the ratio of ^{235}U to ^{238}U in our laboratory sample of uranium ore UNO_3 (called "yellow cake"). To carry out this measurement, begin by understanding the decay chains of ^{235}U and ^{238}U. Radioactive decays from this sample include three radiation types, α, β,

and γ. From the measured energy spectrum, decide which decays from a specific isotope and specific level are visible and should be present only once in the decay scheme. Using the determined detector efficiency, determine the ratio $N(235)/N(238)$ to measure the relative uranium isotope abundance of A=235 to A=238. Is it the ratio expected from the normal isotopic abundance found in nature? Is the source in our laboratory an enriched 235 sample or a depleted 235 sample?

TECHNICAL REPORT PREPARATION

The following sections should be included in the Technical Report.

a). **Abstract** - The abstract should be a very short and concise description of what is in the report. Its purpose is to help others who may be looking up the literature on a particular subject. The researcher should be able to read the abstract in a matter of seconds and discern the salient details and results of the report.

b). **Theory** - This section should contain a complete exposition of the theory discussing the physical phenomena and the equations behind the experiment. A proper derivation of the formulas used in the experiment must be included. The theory should be relevant and complete. Any relevant figures should be included.

c). **Experimental Details** - This section should include a complete description of the experiment and all equipment used. A schematic drawing of the equipment and/or any critical components must be included.

d). **Data** - The data from the experiment must be included, organized into tables with the quantity and its units given. Be consistent and correct with significant figures. This section must also include a complete detail of all statistical and systematic uncertainties in the data along with a complete description of how they were determined or assigned.

e). **Results** - Detailed analysis of the measured data should be included here. The various calculated values should be included here in tabular form. All data should be plotted on graphs with both axes clearly labeled. Any relevant fits to the data should be included here and the results discussed in full.

f). **Conclusions** - The conclusions should contain a summary of the outcome of the experiment (e.g. what was learned), calculated values, mathematical statement of errors, and an interpretation of graphs and tables. The conclusions reached as to verification of theory and a detailed discussion of the causes and the elimination of errors should also be included. Suggestions about improvements, further research, and other remarks should also be made. The conclusion is important and should show considerable thought about the experiment.

g). **Bibliography** - Any and all references that have been used in the preparation of the report should be listed here. An example of a bibliography item is:

P.A. Tipler, *"Physics for Scientists and Engineers"*, (Freeman-Worth, New York, 1999), pp. 1284.

Note: It is good for the student to look at textbooks to see how equations, graphs, figures, and tables are handled and displayed. These are good models to use.

Germanium Detectors

Discrete-line γ-ray spectroscopy requires a detection system that offers excellent energy resolution. Today, practically all γ ray spectroscopy experiments employ high-resolution germanium (Ge) detectors. The germanium detector, similar to other semiconductor detectors, is a large reverse-biased p-n junction diode. At the junction between the p-type and the n-type material, the migration of electrons from the n-type material and holes from the p-type material gives rise to a region of net zero charge. This region is known as the *depletion region.* The net positive charge on one side of the junction, and the net negative charge on the other, sets up an electric field gradient across the depletion region. Any γ rays interacting with the germanium (through the photoelectric effect, Compton scattering, or pair production) will produce electron-hole pairs in the depletion region, which will then be swept to the edges of the detector because of the electric field gradient, constituting an electric current. Since the depletion region is the active part of the Ge detector, the active volume is required to be as large as possible. If a reverse-bias is applied, the width of the depletion region can be increased. The width is proportional to $(V/n)^{1/2}$. Here, V is the bias voltage applied and n is the impurity concentration of the germanium. Natural purity germanium can only maintain a depletion region of a few millimeters before electrical breakdown occurs. Therefore at a given bias voltage, the only way to increase the width of the depletion region is to reduce the impurity concentration, N. This fact led to the introduction of *lithium-drifted* germanium detectors known as Ge(Li) detectors. These detectors are manufactured by adding lithium donor atoms to the Ge material. The donor lithium atoms exactly balance the acceptor impurities, resulting in a very low net impurity level. This allows the depletion region to be extended over the whole of the lithium-drifted region. Advances in manufacturing techniques have, however, allowed extremely pure Ge crystals to be grown. This *high-purity germanium*, or HPGe, has impurity concentrations of around one part in 10^{12}, allowing depletion depths of several centimeters to be achieved. High-purity germanium also has the advantage over Ge(Li), in that it can be stored at room temperature. Ge(Li) detectors must be stored at 77K, to avoid a redistribution of the drifted lithium, which effectively destroys the detector.

The energy required to create an electron-hole pair in Ge is approximately 3 eV, thus an incident γ ray, with an energy of several hundred keV, produces a large number of such pairs, leading to good resolution and low statistical fluctuations. These are desirable properties. HPGe detectors are operated at temperatures of around 77 K, in order to reduce noise from electrons that may be thermally excited across the small band gap in Ge (0.67 eV) at room temperature. This is achieved through thermal contact of the Ge crystal with a dewar of liquid nitrogen, using a copper rod, known as a cold finger.

The contribution from the detector to the overall resolution can be calculated from the formula:

$$\text{system resolution} = \sqrt{[R(d)]^2 + [R(E)]^2}, \tag{1}$$

where $R(d)$ is the detector resolution and $R(E)$ is the electronic resolution. These resolutions add in quadrature. There is a lower limit to $R(d)$ that is energy dependent. The production

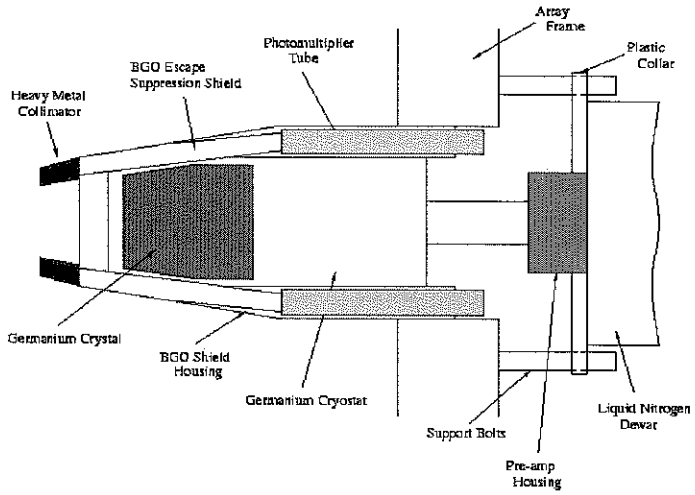

Figure 1: Schematic diagram of a typical germanium detector showing the germanium crystal, the photomultiplier tube, and the liquid nitrogen cooling system.

where $R(d)$ is the detector resolution and $R(E)$ is the electronic resolution. These resolutions add in quadrature. There is a lower limit to $R(d)$ that is energy dependent. The production of electron-hole pairs is a process that is statistical in nature, and hence there are fluctuations in the actual number produced. When the proper statistics are used, the theoretical lower limit to $R(d)$ is given by:

$$R(d) = K\sqrt{F \cdot E}, \tag{2}$$

where K is a constant, E is the energy of the photon in MeV, and F is the statistical Fano factor (a measure of the magnitude of the statistical fluctuations). To a very good approximation, this equation reduces to:

$$R(d) \text{ in keV} = 1.44\sqrt{E \text{ (in MeV)}}. \tag{3}$$

Acknowledgements

The material in this document has been extracted from a thesis from P.T. Greenless at the University of Liverpool and Ortec Application Note AN-34.

Experiment Layout

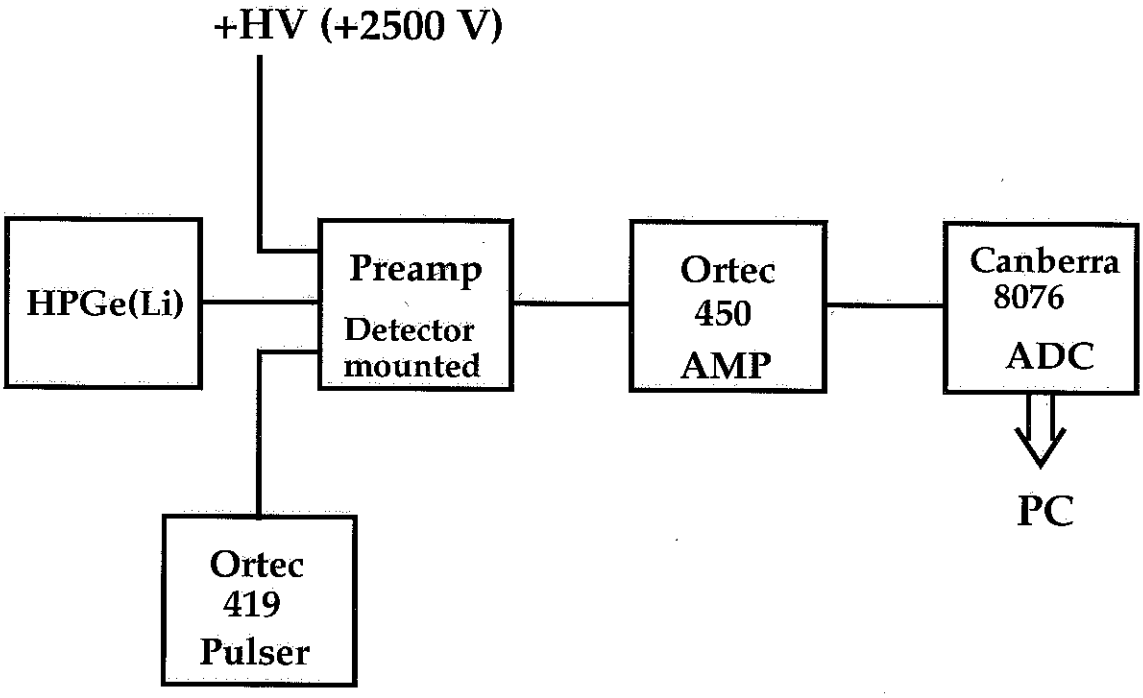

Electronics Modules List

572

- **Ortec 450 Research Amplifier** : This amplifier is designed for use with pulse-type radiation detectors and for amplification of any frequency spectrum within bandwidth limits.

459

- **Ortec 456 High Voltage Power Supply** : This high voltage power supply provides either polarity output voltage from 50 to 3000 V and current from 0 to 10 mA.

- **Ortec 419 High Precision Pulse Generator** : This pulse generator is used to inject a narrow pulse into a semiconductor or scintillator detector.

- **Canberra 8076 ADC** : This analog-to-digital converter generates a digital word proportional to the amplitude of an input pulse. The ADC digitizes the output signal from the Research Amplifier such that the output pulse is directly proportional to the energy of the incident radiation.

Interactions of Gamma Rays with Matter

The total attenuation coefficient for a gamma ray or x-ray traveling through a medium has contributions from scattering, photoelectric absorption, and pair production processes. For the purposes of this work, photonuclear and other such small effects are neglected. These three main processes are discussed below.

1 Compton Scattering

Figure 1 shows schematically the process of Compton scattering. In this case an incident gamma ray scatters from an outer shell electron in the absorber material at an angle θ, and some of the gamma ray energy is imparted to the electron.

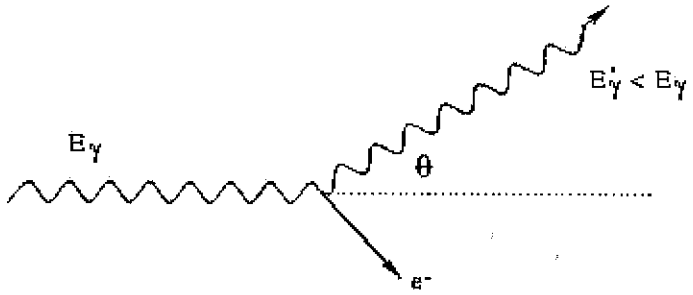

Figure 1: The process of Compton scattering.

Conservation of energy and momentum leads us to the following expression for the energy of the scattered photon:

$$E'_\gamma = \frac{E_\gamma}{1 + (E_\gamma / m_0 c^2)\,(1 - \cos\theta)}, \tag{1}$$

where E_γ is the incident photon energy, E'_γ is the energy of the scattered photon, $m_0 c^2$ is the electron rest mass energy. The kinetic energy of the electron after the collision is given by:

$$T_e = E_\gamma - E'_\gamma = \frac{E_\gamma^2\,(1 - \cos\theta)}{m_0 c^2 + E_\gamma\,(1 - \cos\theta)}. \tag{2}$$

It can be seen that, since all scattering angles are possible, the electron energy ranges from zero for $\theta = 0°$ to $2E_\gamma^2/(m_0 c^2 + 2E_\gamma)$ for $\theta = 180°$, and that the photon never loses the whole of its energy in any one collision. The scattered photon can then continue through the absorber and interact again or scatter out of the absorber material completely. This process, where the scattered photon escapes, is very important for the γ-ray spectroscopist. If the full energy of the incident photon is not absorbed in the detector, then there is a continuous background in the energy spectrum, known as the Compton continuum. This continuum

extends up to an energy corresponding to the maximum energy transfer, where there is a sharp cut-off point, known as the Compton edge.

Compton scattering is the most probable process for photons in the intermediate energy range and the probability decreases rapidly with increasing energy. The probability is also dependent on the number of electrons available for the photon to scatter from, and hence increases with increasing Z.

2 Photoelectric Absorption

The process of photoelectric absorption is shown in Fig. 2. Here an incident photon is completely absorbed by an atom in the absorber material, and one of the atomic electrons is ejected. This ejected electron is known as a photoelectron. The electron must be bound to the atom, to conserve energy and momentum. The kinetic energy of the photoelectron is given by:

$$T_e = E_\gamma - B.E., \tag{3}$$

where $B.E.$ is the binding energy of the atomic electron. The vacancy left in the atomic structure by the ejected electron is filled by one of the electrons from a higher shell. This transition is accompanied by an emission of an x-ray. These x-rays are also absorbed by the detector. Photoelectric absorption is the most favorable process for the γ-ray spectroscopist, since the incident photon deposits all of its energy into the detector, but it is only dominant for low energy photons (<200 keV). The interaction is again dependent upon Z, and an approximate expression for the absorption probability τ is:

$$\tau \propto \frac{Z^n}{E_\gamma^{3.5}}. \tag{4}$$

Here n is normally between 4 and 5 depending on the absorber material. This dependence on Z explains the choice of high-Z materials (such as lead) for shielding purposes.

Figure 2: The process of photoelectric absorption.

3 Pair Production

The third important gamma ray interaction is the process of pair production, shown in Fig. 3. If the incident photon energy is greater than 1.022 MeV (twice the electron rest mass energy) in the presence of an atomic nucleus an electron/positron pair can be produced. Any residual energy is distributed evenly between the electron and positron as kinetic energy. As the positron slows to thermal energies through interaction with the absorbing medium, it can annihilate with one the atomic electrons producing two gamma rays of energy 511 keV. These gamma rays can then either be absorbed or escape the detector. This is evidenced by the so-called *escape peaks* observed in gamma ray spectra. If one of the 511 keV photons escapes the detector, then a peak is observed at: $E_\gamma - m_0c^2$ (single escape peak). If both escape, then a peak is observed at $E_\gamma - 2m_0c^2$ (double escape peak). The process of pair production only becomes important for high energy gamma rays (5 - 10 MeV) that are outside the energy range of interest in the present work.

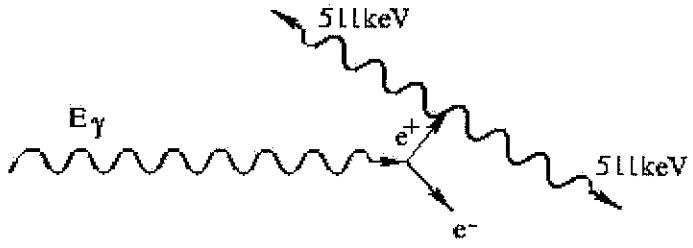

Figure 3: The process of pair production/annihilation.

Acknowledgements

Much of the material in this document has been extracted from the thesis of P.T. Greenless at the University of Liverpool and Ortec Application Note AN-34.

Section 6
Detector Specifications and Performance Data

6.1 SPECIFICATIONS Model Number GR1020 Serial Number 5871624

The purchase specifications and therefore the warranted performance of this detector are as follows:

Rel. Efficiency - 10 %

Resolution - 2.0 keV (FWHM) @ 1.33 MeV

- _____ keV (FWTM) @ 1.33 MeV

- _____ keV (FWHM) @ _____

- _____ keV (FWTM) @ _____

Peak/Compton - _____ :1

Cryostat Description or Drw. No. if special 7600

6.2 PHYSICAL/PERFORMANCE DATA

Actual performance of this detector when tested is given below.

Geometry Reverse electrode closed ended coaxial

Diameter 44.6 mm

Length 36 mm

Active area facing window 15.8 cm^2

Distance from window 5 mm

Electrical Characteristics

Depletion Voltage (-)3000 V dc.

Recommended Bias Voltage (-) 4000 V dc.

Leakage Current at Recommended Bias 0.04 Na.

Preamplifier Test Point Voltage at Recommended Bias (-) 1.60 V dc.

Capacitance at Recommended Bias ~17 pf.

Resolution and Efficiency - with Amp Time Constant of 4 microseconds.

Isotope	Co^{57}	Co^{60}			Cd^{109}
Energy (keV)	122	1332			Ratio 22/88keV
FWHM (keV)	0.72	1.73			
FWTM (keV)	1.32	3.21			
Peak/Compton		49:1			
Efficiency (%)		13.8			>23:1

U. S. Department of Commerce
Malcolm Baldrige
Secretary

National Bureau of Standards
Ernest Ambler, Director

WHICH IS BEING MAILED TO YOU UNDER SEPARATE COVER.

National Bureau of Standards

Certificate

Standard Reference Material 4275-B

MIXED-RADIONUCLIDE POINT-SOURCE STANDARD
for the
EFFICIENCY CALIBRATION OF GERMANIUM-SPECTROMETER SYSTEMS

Antimony-125-Tellurium-125m
Europium-154
Europium-155

Source identification	SRM 4275-B - 43
Source description	Point source on polyester tape (1)*
Reference time	1200 EST May 1, 1983

This standard is intended for use in measuring the full-energy-peak efficiencies of spectrometer systems for x and gamma rays from 27 to 1596 keV, provided that the responses to radiations approximately 5 keV apart can be resolved. Emission rates are specified at 19 energies for photon radiations from a mixture of antimony-125-tellurium-125m, europium-154, and europium-155. Uncertainties are estimated and combined at a level corresponding to a standard deviation of the mean, with the intent that the user can propagate this uncertainty along with the other uncertainties in the spectrometer calibration.

Table 1 gives the energies, emission rates, and uncertainties for selected radiations. A footnote indicates how emission rates will change with time. If there are any changes in measured emission rates that would correspond to an emission rate 0.5 percent different from that calculated from Table 1, or in measured half lives that would cause a corresponding difference after five years, notification will be sent to purchasers of the standard.

Table 2 lists the estimates of component uncertainties which have been combined in quadrature to give the total uncertainty in each emission rate.

Notes on the use of this standard are appended. One of the tables in the supplemental notes gives relative emission rates for radiations close in energy to the certified radiations; for spectrometer systems of poorer resolution, it may be necessary to use a combined emission rate for some multiple peaks.

This Standard Reference Material was prepared in the Center for Radiation Research, Nuclear Radiation Division, Radioactivity Group, Dale D. Hoppes, Group Leader.

Washington, D.C. 20234
July, 1983

Stanley D. Rasberry, Chief
Office of Standard Reference Materials

*Footnotes on page 4

X-Ray and Gamma-Ray Energies, Emission Rates [2,3], and Uncertainties for Standard Reference Material 4275-B

TABLE 1

Radionuclide	Photon Energy (keV)	Emission Rate ($\times$ s^{-1}) or (γ s^{-1}) 1200 EST May 1, 1983	Total Estimated Uncertainty (%)*
^{125}Sb - ^{125m}Te	Kα, 27.4	1.283×10^{4}	1.3
^{154}Eu - ^{155}Eu	Kα, 42.8	9.537×10^{3} (4)	1.3
1 ^{155}Eu	86.6	5.471×10^{3}	0.8
2 ^{155}Eu	105.3	3.779×10^{3}	1.1
3 ^{154}Eu	123.1	1.307×10^{4}	0.7
4 ^{125}Sb	176.4	1.408×10^{3}	0.6
5 ^{154}Eu	248.0	2.215×10^{3}	0.6
6 ^{125}Sb	380.5	3.120×10^{2}	0.8
7 ^{125}Sb	427.9	6.118×10^{3}	0.7
8 ^{125}Sb	463.4	2.151×10^{3}	0.7
9 ^{154}Eu	591.7	1.585×10^{3}	0.6
10 ^{125}Sb	600.6	3.634×10^{3}	0.6
11 ^{125}Sb	635.9	2.322×10^{3}	0.6
12 ^{154}Eu	723.3	6.434×10^{3}	0.6
13 ^{154}Eu	873.2	3.905×10^{3}	0.7
14 ^{154}Eu	996.4	3.343×10^{3}	1.0
15 ^{154}Eu	1004.8	5.795×10^{3}	0.7
16 ^{154}Eu	1274.4	1.117×10^{4}	0.6
17 ^{154}Eu	1596.5	5.678×10^{2}	0.7

* Estimated total uncertainties have the significance of one standard deviation of the mean. Components of these estimates are given in Table 2.

Estimates of the Component Uncertainties for Photon-Emission-Rate Values for SRM 4275-B

TYPICAL UNCERTAINTY COMPONENTS (%)

TABLE 2

Photon Energy (keV)	Number of Determin-ations	Std. Dev. of the Mean	Effici-ency	Peak Analysis	Pile-up Compen-sation	Geometry	Other*	Overall Uncer-tainty**
27.4	6	0.3	1.0	0.7	0.3	0.1	0.2	1.31
42.8	6	0.06	1.0	0.7	0.1	0.1	0.5	1.3
86.6	6	0.12	0.65	0.3	0.1	0.1	0.05	0.74
105.3	6	0.09	1.0	0.3	0.1	0.1	0.05	1.1
123.1	6	0.08	0.6	0.4	0.1	0.08	0.05	0.74
176.4	6	0.09	0.5	0.2	0.2	0.1	0.05	0.59
248.0	6	0.04	0.5	0.3	0.1	0.08	0.05	0.60
380.5	6	0.36	0.7	0.2	0.2	0.08	0.05	0.84
427.9	6	0.23	0.7	0.2	0.2	0.08	0.05	0.79
463.4	7	0.22	0.58	0.2	0.2	0.08	0.05	0.69
591.7	6	0.12	0.45	0.3	0.1	0.08	0.05	0.57
600.6	7	0.20	0.42	0.4	0.2	0.08	0.05	0.65
635.9	6	0.19	0.42	0.2	0.2	0.08	0.05	0.55
723.3	6	0.05	0.54	0.2	0.1	0.08	0.05	0.59
873.2	5	0.12	0.63	0.3	0.1	0.08	0.05	0.72
996.4	5	0.11	0.54	0.75	0.1	0.08	0.05	0.94
1004.8	5	0.06	0.54	0.4	0.1	0.08	0.05	0.69
1274.4	5	0.06	0.45	0.1	0.1	0.08	0.05	0.46
1596.5	6	0.43	0.40	0.1	0.2	0.15	0.05	0.64

* Includes contributions for the half lives for the Te x-ray, for the decay schemes for Gd x-ray, and for gravimetric factors in the source preparation.

** Components of the uncertainty have been added in quadrature. This is the overall uncertainty for a typical detector, and some of the values are slightly greater than those given in the last column of Table 1.

UNITED STATES DEPARTMENT OF COMMERCE
National Bureau of Standards
Washington, D.C. 20234

NOTES ON THE USE OF STANDARD REFERENCE MATERIALS 4275-B AND 4276-B

MEASURING EFFICIENCIES OF GERMANIUM SPECTROMETER SYSTEMS WITH NBS LONG-LIVED MIXED-RADIONUCLIDE STANDARDS

1. Introduction

Careful measurements with many calibrated single-radionuclide sources may give the most accurate efficiency-energy relations for germanium spectrometers, but the use of one source with established photon (gamma-ray or x-ray) emission rates at many energies often suffices and is more convenient. There is a further convenience if the radionuclides involved are long-lived, for experience has shown that system efficiencies should be checked periodically.

Inevitably, there are compromises in the composition of such standards, especially if they are to have a sufficient density of photon energies to define the calibration relation without a strong dependence on an assumed analytic relation. In selecting the components for the present long-lived mixed radionuclide standard, we considered the balance of emission rates at significant energies, spectral conflicts, source attenuation, simplicity in use, correlated summing, calibration difficulties, and the cost and availability of the radionuclides.

The standard is composed of ^{125}Sb (with ^{125m}Te in equilibrium), ^{154}Eu, and ^{155}Eu. Photon-emission rates for the major radiations have been measured with four germanium spectrometer systems especially calibrated for the purpose. These emission rates are specified with total uncertainties of from 0.6 to 1.3 percent, estimated to correspond to one standard deviation of the mean. The goal was to provide the users of the standards with a "realistic" uncertainty (as opposed to one which is very conservative) that can be combined with others entering into detector calibrations (such as those from counting statistics, geometry and rate differences, correlated summing, and peak evaluation) to generate an overall uncertainty for their calibration curves.

New information will be supplied to purchasers whenever we have reason to believe that an emission-rate value is different from that stated by 0.5 percent, or when the accuracy has improved significantly.

These standards supply many useful calibration points between 27 and 1596 keV, with other long-lived NBS standards such as ^{60}Co, ^{133}Ba, ^{152}Eu, ^{207}Bi, and ^{228}Th (plus progeny) available to fill in sparse regions and extend the calibrations to higher energies, if that is required. Standards of ^{22}Na, ^{54}Mn, ^{88}Y, and ^{139}Ce are also often available.

We will now describe some points that should be considered in using the standards, and in applying gamma-ray spectrometry in general. A biblography at the end of the report lists a few significant references, some of which describe the techniques used in the gamma-ray emission rate measurements for these standards.

2. Calculation of Emission Rates at Later Times

The half lives of only ^{125}Sb, ^{154}Eu, and ^{155}Eu are involved in the calculation. However, the gadolinium x rays, which supply a useful calibration point for good-resolution detectors, result from both ^{154}Eu and ^{155}Eu decays and hence the calculation involves the sum of two components, as shown on the certificate notes. The half lives and uncertainties (from an unweighted average of recent values from 2 or 3 laboratories) are: ^{125}Sb - 1008.7 ± 1.0 days; ^{154}Eu - 3127 ± 8 days; and ^{155}Eu - 1741 ± 10 days.

We will continue to monitor the emission rate of pure samples of each radionuclide, and report to the purchasers any change that would make a difference of greater than 0.5 percent after 5 years.

3. Spectral Conflicts

A complete list of the more than 200 gamma rays reported for this mixture would discourage any consideration of using such sources as efficiency-calibration standards, but an examination of spectra (as shown in Figures 1 and 2) shows that there are about 20 dominant peaks, with few serious energy conflicts for good resolution detectors and few background difficulties (Compton edges or backscatter peaks) that interfere with peak-area analyses to more than one percent. For poorer-resolution detectors, the contributions of weak peaks in the 176-keV region must be considered, and the analysis of the triad at about 600 keV and the doublet at 1 MeV will present a challenge if the peaks are analyzed separately. However, a simple summing of channel contents, after an interpolated or extrapolated background has been subtracted, can give areas accurate to about 2 percent, for energies of 87 keV or greater. For all systems, the challenge of constructing a consistent and smooth calibration curve, within the uncertainties shown on the emission-rate table, may prove informative about techniques and uncertainties. We are investigating better analysis techniques, and would be interested in non-abusive user comments if discrepancies are found.

Above 120 keV, the accuracy of some NBS emission-rate values appear to be limited by peak analysis uncertainties rather than efficiency uncertainties for our detectors. Below 120 keV, the converse is true for gamma rays, with the paucity of reliable efficiency points making interpolations less certain. For the x rays, the deviation of our measured K_α to K_β rations from literature values indicates that peak-area measurements are less reliable for these radiations at the present time, and this is reflected in the uncertainties quoted.

Table 1 lists the dominant photon energies, and suggests where conflicts may occur. The probablity of interfering gamma rays, relative to the probability of the dominant gamma ray, are from NBS measurements, or literature values for some very small contributions. Users can judge if conflicts are significant for their system resolution and their required uncertainties, and make corrections (some of which change with time) if necessary.

4. Pulse-Summing Corrections

When two radiations strike a germanium detector within the shaping time of the amplifier, one or both can fail to be recorded in channels where they would have been otherwise. This time coincidence may occur because of an accidental overlap of pulses resulting from the decay of two separate nuclei, or it may arise from the detection of nearly simultaneous cascade radiations in the decay of the same nucleus.

In the former case of the accidental pile-up of pulses, the rate-dependent losses can be monitored with a constant-rate-pulser peak or almost accounted for with a pile-up rejector and live-time circuit. The live timer of a slow multi-channel analyzer may provide a partial compensation, but this should not be assumed for total rates, above amplifier noise, of more than a few hundred counts per second.

The effect of correlated or cascade summing due to cascade radiations is not rate-dependent but depends on the efficiencies of the detector for the radiations involved, and can result in either the gain or loss of peak counts, depending on the decay scheme of a particular radionuclide.

If a gamma-ray transition competes with two cascade lower-energy gamma rays connecting the same two levels, the peak due to the "crossover" gamma ray may be enhanced by the "summing in" of counts due to correlated gamma-ray pairs which deposit the same energy in the detector. In general the effect is small because the product of peak efficiencies is small compared with the peak efficiency of the crossover gamma ray. (The peak efficiency, ε_p, is defined here as the fraction of all emitted gamma rays which are recorded in a full-energy spectral peak.) But, if the crossover gamma-ray probablility is much lower than that of those summing, the effect can be significant. This is true for the 1596-keV gamma ray in the decay of ^{154}Eu, and corrections will have to be applied for accurate efficiency determinations even with moderate separations between detector and source.

If "summing in" occurs, the total peak area, compared to what it would have been otherwise, is $1 + [\, K(a,b,c)\varepsilon_p(a)\varepsilon_p(b)/\varepsilon_p(c)]$, where indices a and b represent the cascade gamma rays and c represents the crossover, and $K(a,b,c)$ is the probability for the a and b gamma rays to be emitted in cascade relative to the probability for the emission of c. If more than one pair of gamma rays can sum to the crossover energy, other terms like that in the square bracket must be added. Therefore, an observed peak must be divided by $1 + \Sigma[K(a_i,b_i,c)\varepsilon_p(a_i)\varepsilon_p(b_i)/\varepsilon_p(c)]$ in order to get the counts due to c alone. Table 2 contains values of $K(a,b,c)$ which have been calculated for the three radionuclides.

Two factors usually make "summing out" of a peak due to the simultaneous detection of a correlated radiation much more significant. It is not required that the summing pulse is one that otherwise would have been stored in a peak; therefore, the total efficiency (ε_t = the fraction of radiation emitted at a given energy that generates pulses of any size in the system) must be considered. This efficiency is often much greater than the corresponding ε_p, so that it is easy to underestimate the effect if the areas of sum peaks are used as a measure. Secondly, the narrow peaks characteristic of germanium spectrometers suffer losses with any summed pulse, even quite small ones. Summing pulses smaller than those which would correspond to a full-energy peak for correlated radiations can result from Compton or photoelectric interactions in the shielding or can result from partial energy loss or incomplete charge collection in the detector.

It would then appear that the total efficiency would also have to be measured at many energies, but in general it varies slowly with energy above 100 keV, and attenuation in detector housings or added absorbers often reduce it in a calculable way at lower energies. Suggested radionuclides for total-efficiency measurements are ^{125}I, ^{241}Am, ^{109}Cd, ^{139}Ce, ^{137}Cs, ^{54}Mn, ^{60}Co, and ^{88}Y. All of these are issued as NBS standards, which are also useful for determining peak efficiencies. Alternatively, radionuclides can be calibrated with sufficient accuracy for total-efficiency measurements by the user from an efficiency-energy relation established with this long-lived standard at a sufficient distance from the detector that summing is small. Note that the effect of correlated summing may be significant, even for total-efficiency measurements, with ^{125}I, ^{60}Co, and ^{88}Y, if the geometry is tight. In any case, the contribution of x rays and other gamma rays must be removed by subtraction of known lower-energy contributions or extrapolation of the spectrum through low-energy-peak regions. A curve of the total efficiency *vs* energy for a point source at 26 centimeters from a 60-cm^3 wrap-around coaxial germanium detector is shown in Figure 3.

Beta-ray or conversion electron efficiencies may be appreciable if sufficient absorbers are not present, and can also cause "summing out". In most calculations, including the ones we are going to suggest, it is assumed that electrons, and L and higher-shell x rays, are not detected. K x rays often are important, especially in nuclides decaying by K-electron capture.

The peak area for the rth radiation with summing out by radiation s is related to that which would be measured without the effect by $1 - K(s,r)\varepsilon_t(s)$, where $K(s,r)$ is the probability for the simultaneous emission of the two. If there are other summing possibilities, the total effect is not simply $1 - \Sigma K(s_j,r)\varepsilon_t(s_j)$. If the efficiency is large, additional additive terms such as $\Sigma K(s_j s_k r)\varepsilon_t(s_j)\varepsilon_t(s_k)$ can be significant (and possibly analogous terms containing the product of three efficiencies must be subtracted, and so forth). We have calculated all pertinent Ks for these three radionuclides (and many other), and will supply the full set on request. However, the first-order terms given in Table 2 will probably be sufficient unless the source is close to the detector and the required accuracy is high.

There are two further complications. In general, angular correlations between pairs of correlated gamma-rays (not x rays) must be taken into account by introducing factors multiplying each K. For the present radionculides these are sufficiently close to 1 that we do not list them here. This may not be true of other radionuclides that users wish to measure. The second complication is that the discussion so far has been for point sources; if the sources are extended, high accuracy results will require a measurement of ε_t and a calculation of the summing effect at different locations, and then an integration over the volume of the source.

This discourse on summing effects does not appear because these standards are especially troublesome in this respect; quite the opposite is true. (Compare them with ^{166m}Ho!) If users must count at high efficiencies and yet require accuracies of better than 10 percent (or even 50 percent, in extreme cases), there is another alternative to the admittedly laborious summing corrections. They should ignore the concept of an efficiency-energy relation, and calibrate the detector directly in terms of apparent peak efficiency for selected gamma rays of the radionuclides which will be measured. If standards are not available, the radionuclides can be calibrated in the laboratory by establishing an efficiency-energy relation with this standard at a source-detector distance where summing is a fraction of a percent for all radionuclides (probably 25 centimeters or more). Concentrated solutions of the radionuclides (or mixtures thereof) can be calibrated at this distance, using tabulated P_γs and taking into account container and source absorption and other corrections. These solutions can then be quantitatively diluted (to probably better than 1 percent by simple volume measurements, if the initial volume is greater than a few ml) and counted in the usual geometry.

5. Other Gamma Rays

We have intentionally not given emission rates for weaker gamma rays, although many users might find them convenient. In many cases the values have not been measured well, as evidenced by the considerable discrepancy with literature values. If accurate values become available, purchasers of standards will be informed, although our feeling is that more accurate efficiencies will result from using separate standards with less background.

6. Sample Preparation Considerations

The solution SRMs 4276 and 4276-B are provided in 4 M hydrochloric acid, which has a density of 1.06 g cm^{-3} at 23°C. They also contains 30 µg each of Sb^{+3} and Eu^{+3} per gram of solution. A similar carrier solution should be used for dilutions.

If sources of this mixture are to be evaporated to dryness, care must be taken to avoid loss of ^{125}Sb through volatilization. The present point-source standards (SRM 4275 and 4275-B) were prepared by taking to dryness deposited sources in a hydrogen sulfide gas atmosphere such that the antimony is precipitated as the orange Sb_2S_3.

TABLE 1

Considerations for Peak Analysis for SRM's 4275-B and 4276-B

Gamma Ray Energy (keV)	Source	Conflict
27.4	^{125}Sb–^{125m}Te Kα x ray	24.36 keV germanium escape peak from a 35.46 keV γ in ^{125}Sb 26.51 keV γ in ^{155}Eu 0.35% of the 27.4 keV Kαx-ray emission
42.8	^{154}Eu–^{155}Eu Kα x ray	a) see footnotes
86.6	^{155}Eu	86.062 keV γ in ^{155}Eu 0.49% of the 86.6 keV γ emission
105.3	^{155}Eu	104.3 keV backscatter peak of the 176.4 keV γ in ^{125}Sb 109.27 keV γ in ^{125m}Te 0.49% of the 105.3 keV γ emission
123.1	^{154}Eu	122.2 keV Compton edge of the 248.04 keV γ in ^{154}Eu
176.4	^{125}Sb	172.6 keV γ in ^{125}Sb, 3.9% 178.8 keV backscatter peak of the 591.7 keV γ in ^{154}Eu 179.35 keV average backscatter peaks of the 600.6 and 606.7 keV γ's in ^{125}Sb
248.0	^{154}Eu	252.5 keV double-escape peak of the 1274.4 keV γ in ^{154}Eu
380.5	^{125}Sb	a) see footnotes
427.9	^{125}Sb	421.3–426.9 keV Compton edges of the 600.6 and 606.7 keV γ's in ^{125}Sb
463.4	^{125}Sb	a) see footnotes
591.7	^{154}Eu	a) see footnotes
600.6	^{125}Sb	606.7 keV γ in ^{125}Sb. 27.5% of the 600.6 keV γ emission
635.9	^{125}Sb	a) see footnotes
723.3	^{154}Eu	715.8 keV γ in ^{154}Eu 0.89% of the 723.3 keV γ emission, b)
873.2	^{154}Eu	a) see footnotes
996.4	^{154}Eu	1004.8 keV γ in ^{154}Eu 168.9% of the 996.4 keV γ emission, b)
1004.8	^{154}Eu	996.4 keV γ in ^{154}Eu 59.2% of the 1004.8 keV γ emission, b)
1274.4	^{154}Eu	a) see footnotes
1596.5	^{154}Eu	a) see footnotes

a) No significant conflicts are expected for semiconductor detectors of good resolution.

b) Conflicts may depend on specific detector resolution and counting rates.

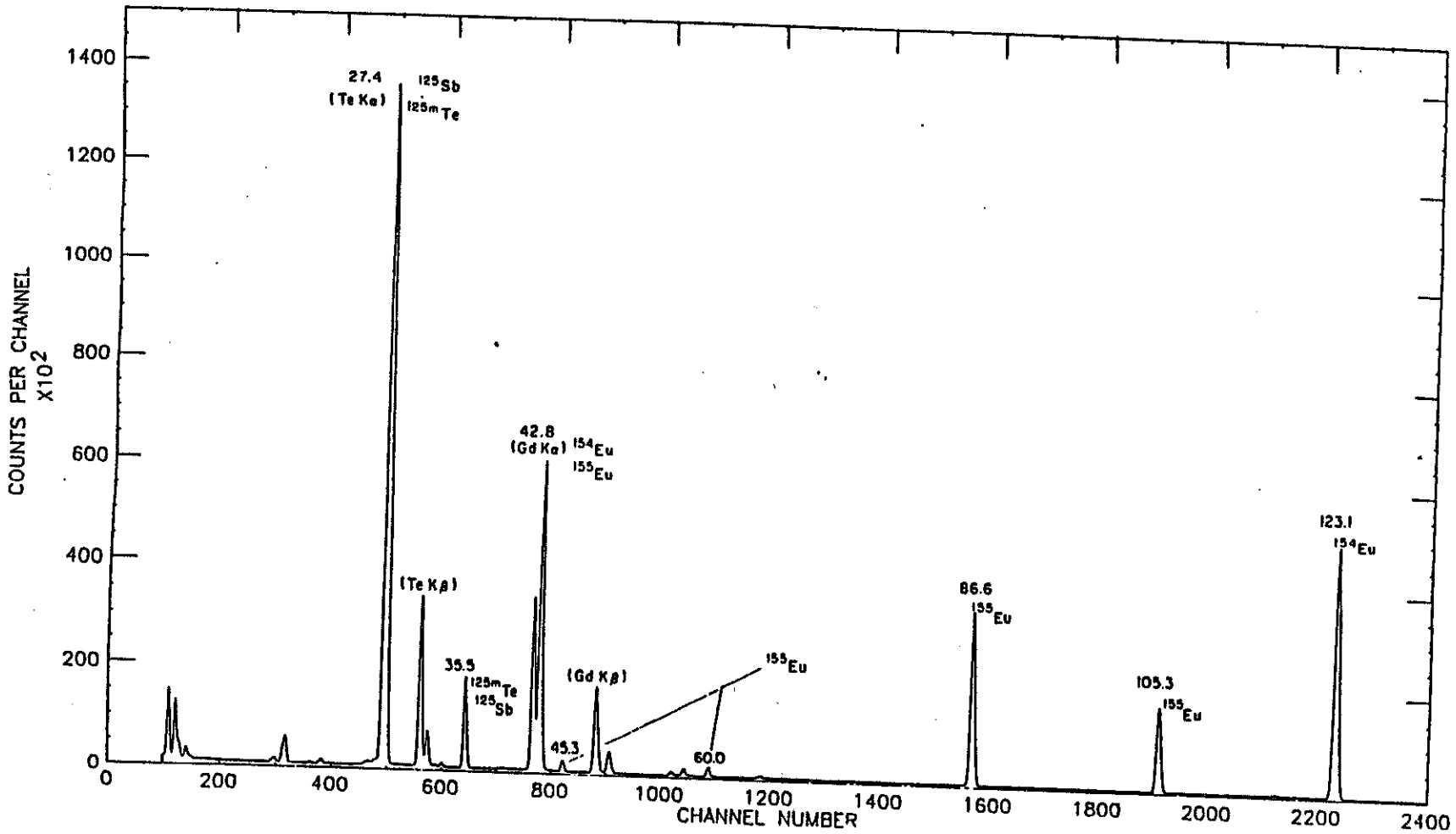

Figure 1. Spectrum of low-energy photons from SRM 4275 taken with a 200-mm^2 area, 5-mm-thick planar germanium detector at a source-to-detector distance of 15 cm.

^{235}U Decay Chain

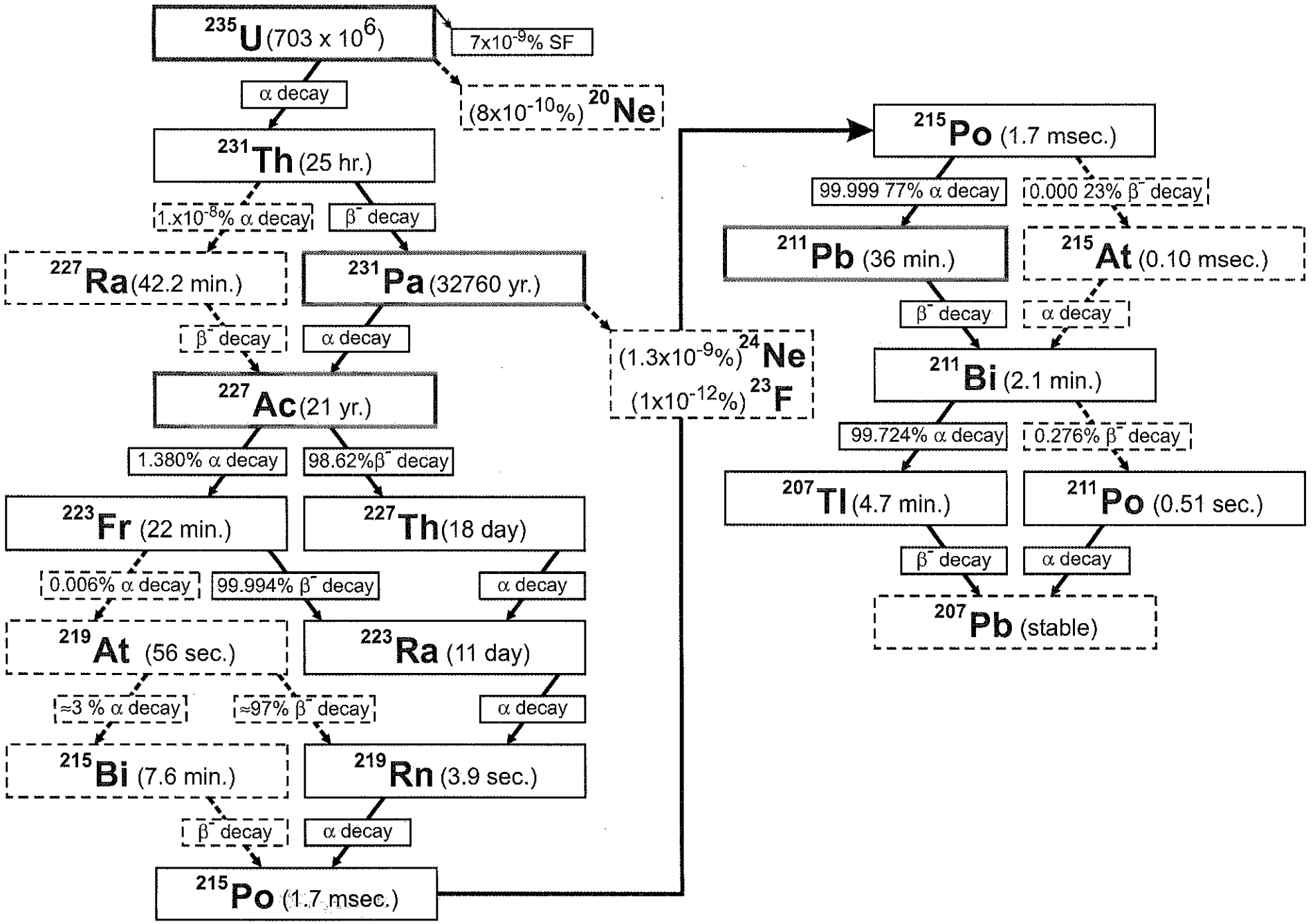

$^{234}_{90}Th_{144}$

^{238}U α Decay

Decay Scheme

Intensities: I(γ+ce)
per 100 parent decays

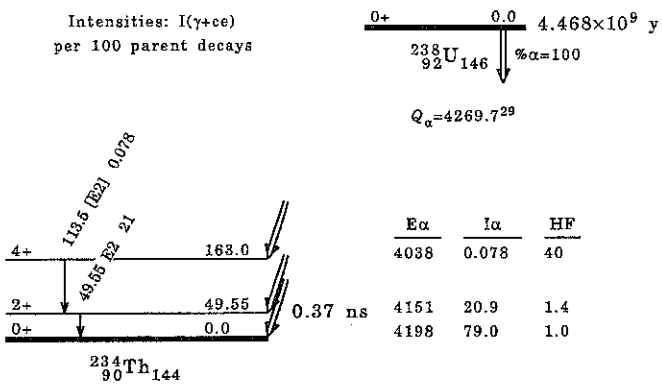

Eα	Iα	HF
4038	0.078	40
4151	20.9	1.4
4198	79.0	1.0

CITATION:
Nuclear Data Sheets (2007)

$^{234}_{91}Pa_{143}$

^{234}Th β- Decay

Decay Scheme

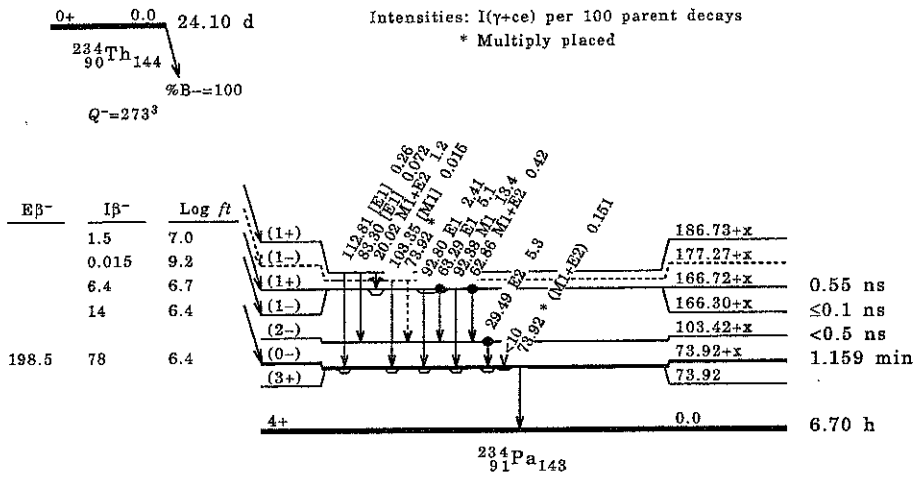

CITATION:
Nuclear Data Sheets (2007)

$^{234}_{92}U_{142}$

^{234}Pa β- Decay (1.159 min) 1975Ar23,1990Sc09 (continued)

Decay Scheme (continued)

(0−) 73.92+x 1.159 min

$^{234}_{91}Pa_{143}$

%B−=99.84 4

Q^-(g.s.)=2195^4

Intensities: I(γ+ce) per 100 parent decays
& Multiply placed; undivided intensity given
@ Multiply placed; intensity suitably divided

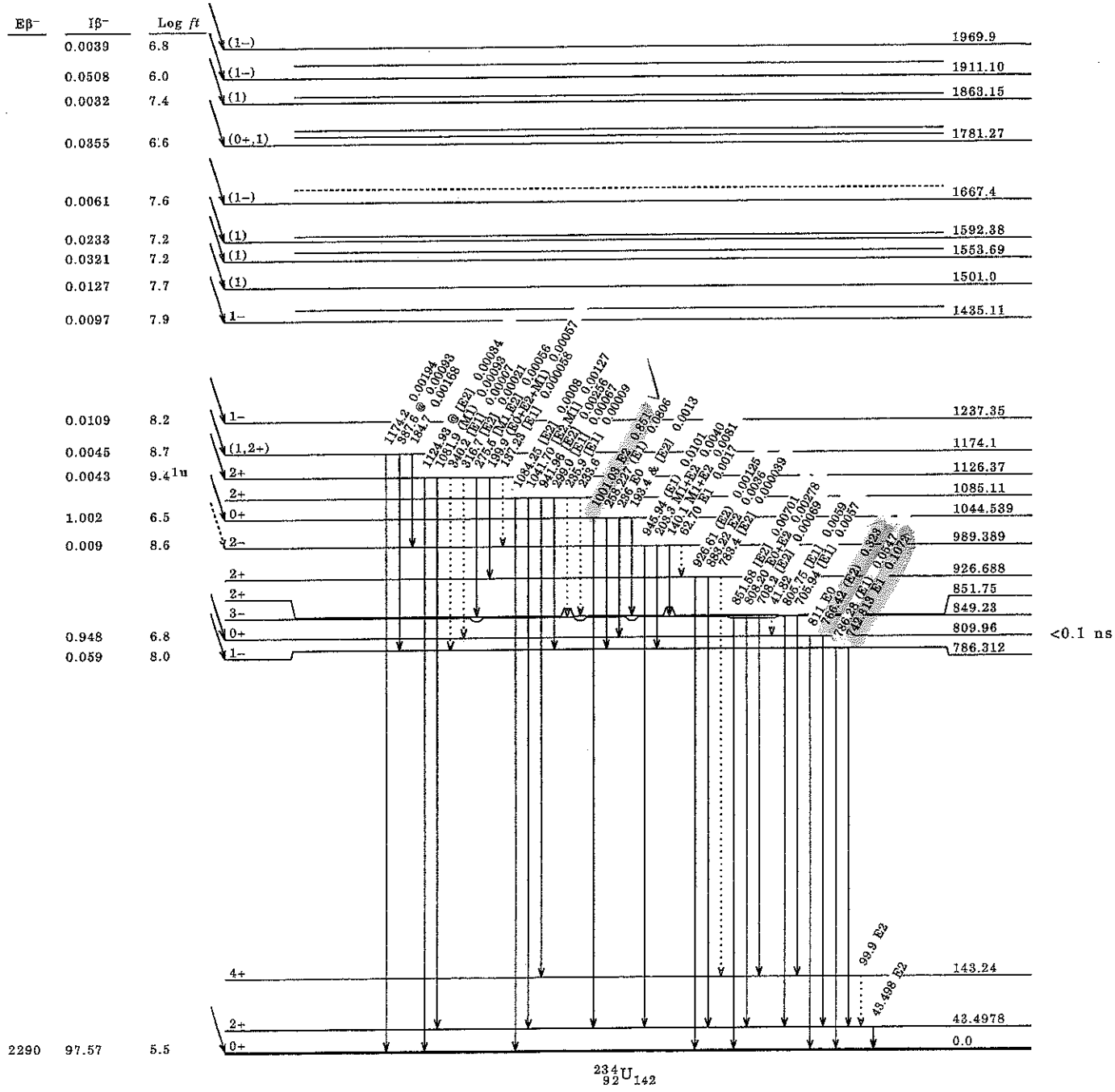

$^{234}_{92}U_{142}$

CITATION:
Nuclear Data Sheets (2007)

$^{234}_{92}U_{142}$

^{234}Pa β- Decay (1.159 min) 1975Ar23,1990Sc09

Decay Scheme

(0-) 73.92+x 1.159 min

$^{234}_{91}Pa_{143}$

%B-=99.84 *4*

Q^-(g.s.)=2195*4*

Intensities: I(γ+ce) per 100 parent decays

& Multiply placed; undivided intensity given

@ Multiply placed; intensity suitably divided

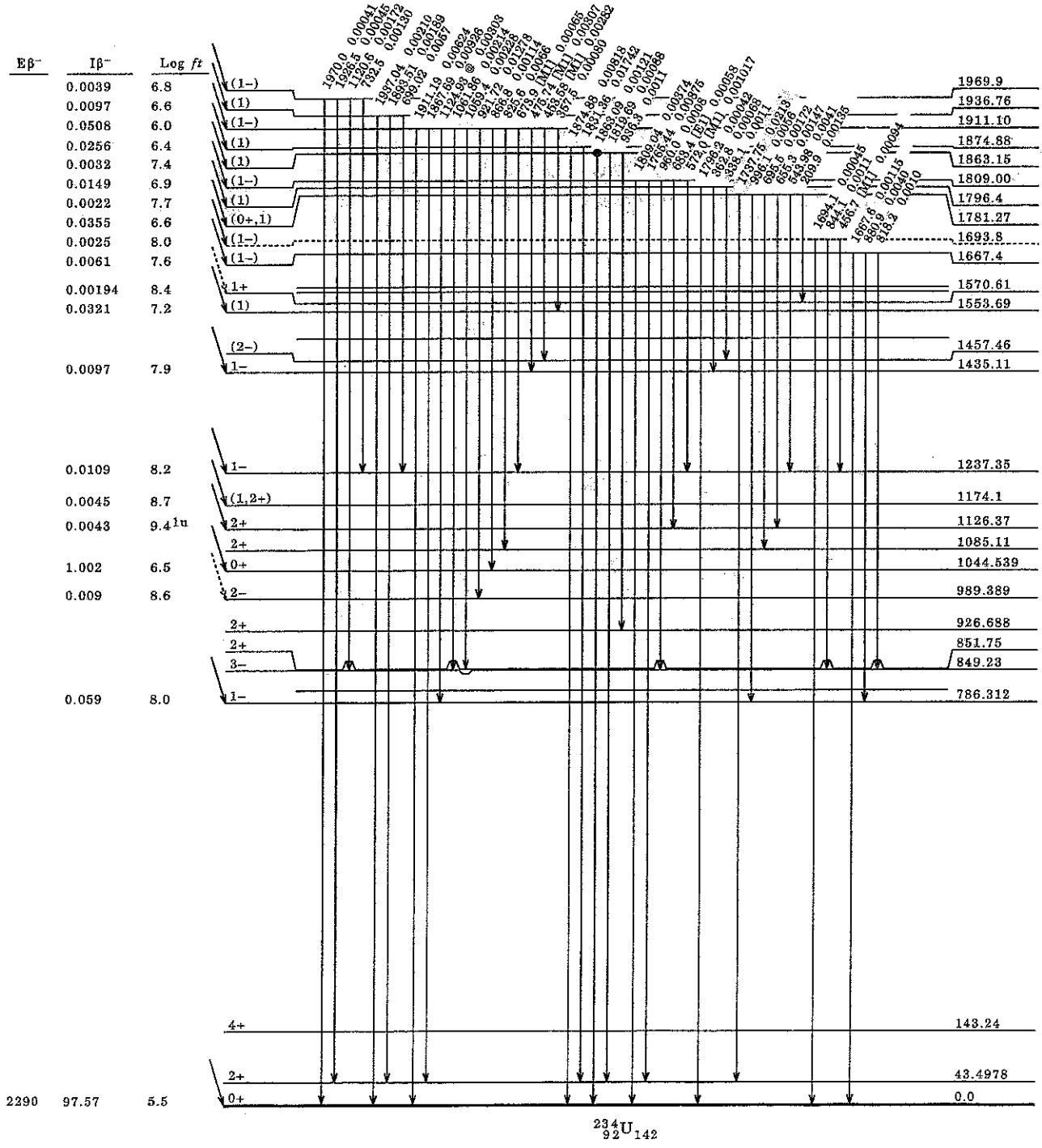

CITATION:
Nuclear Data Sheets (2007)

$^{231}_{90}Th_{141}$

^{235}U α Decay

Decay Scheme

Intensities: I(γ+ce) per 100 parent decays

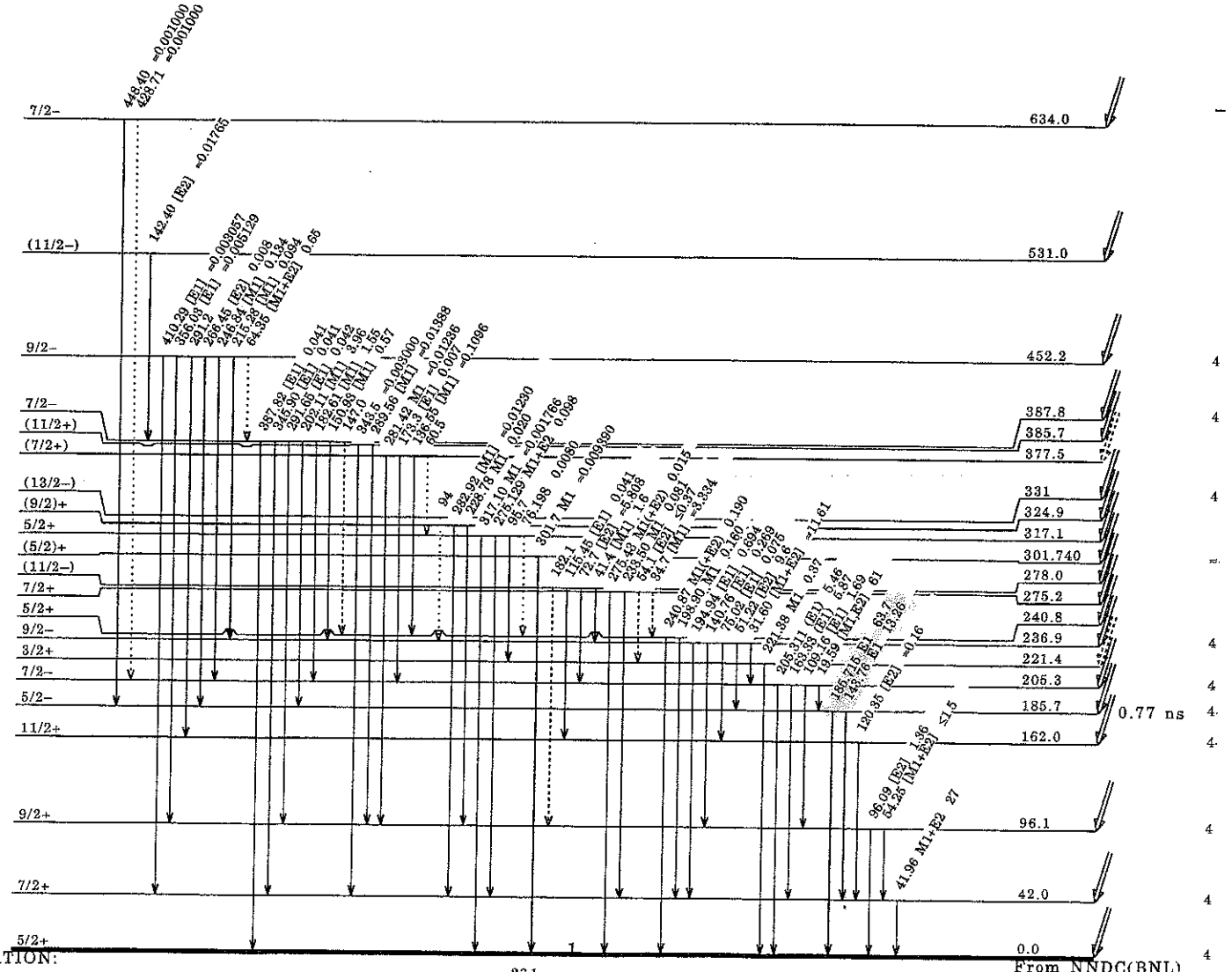

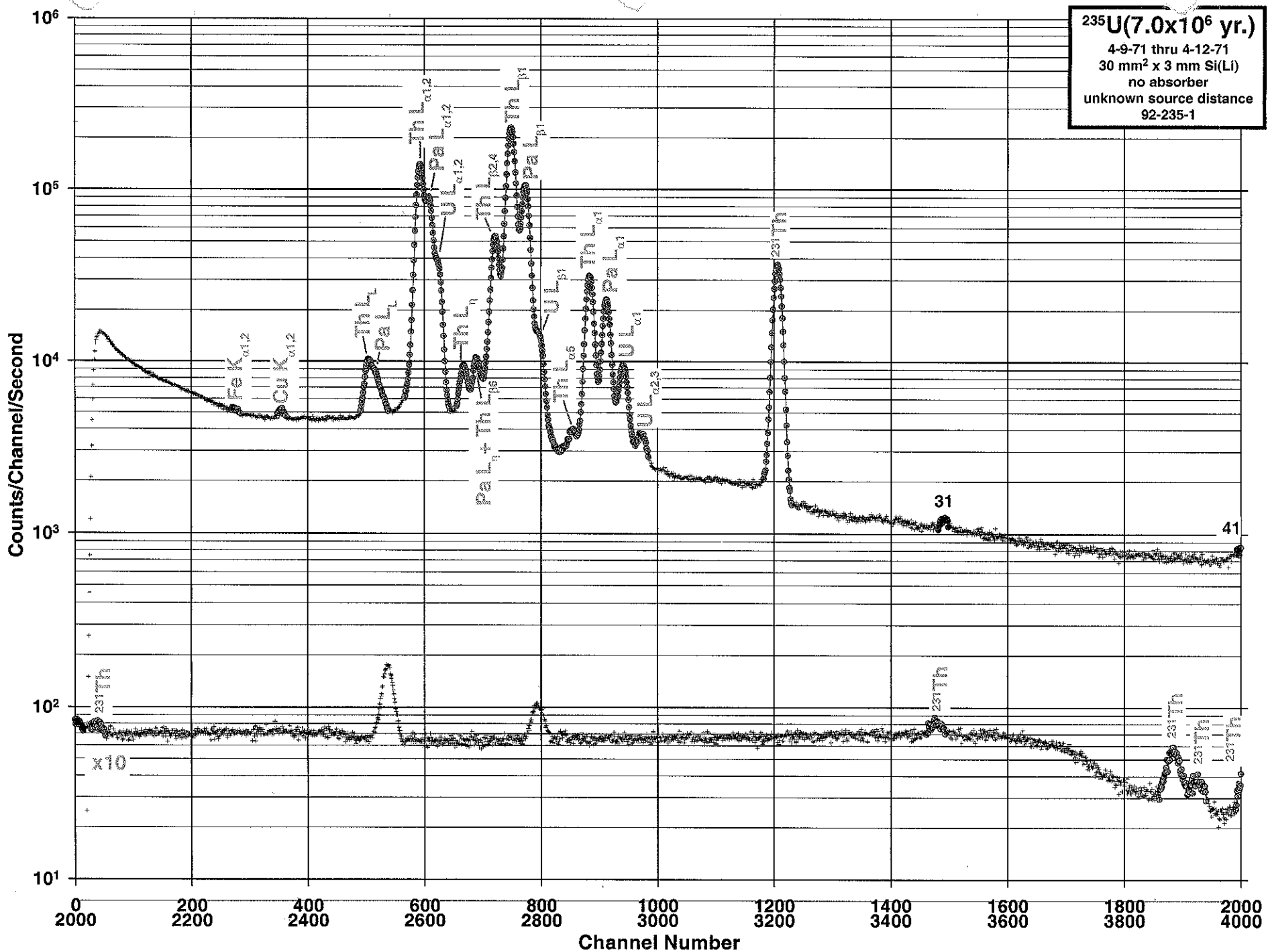

Table of Contents

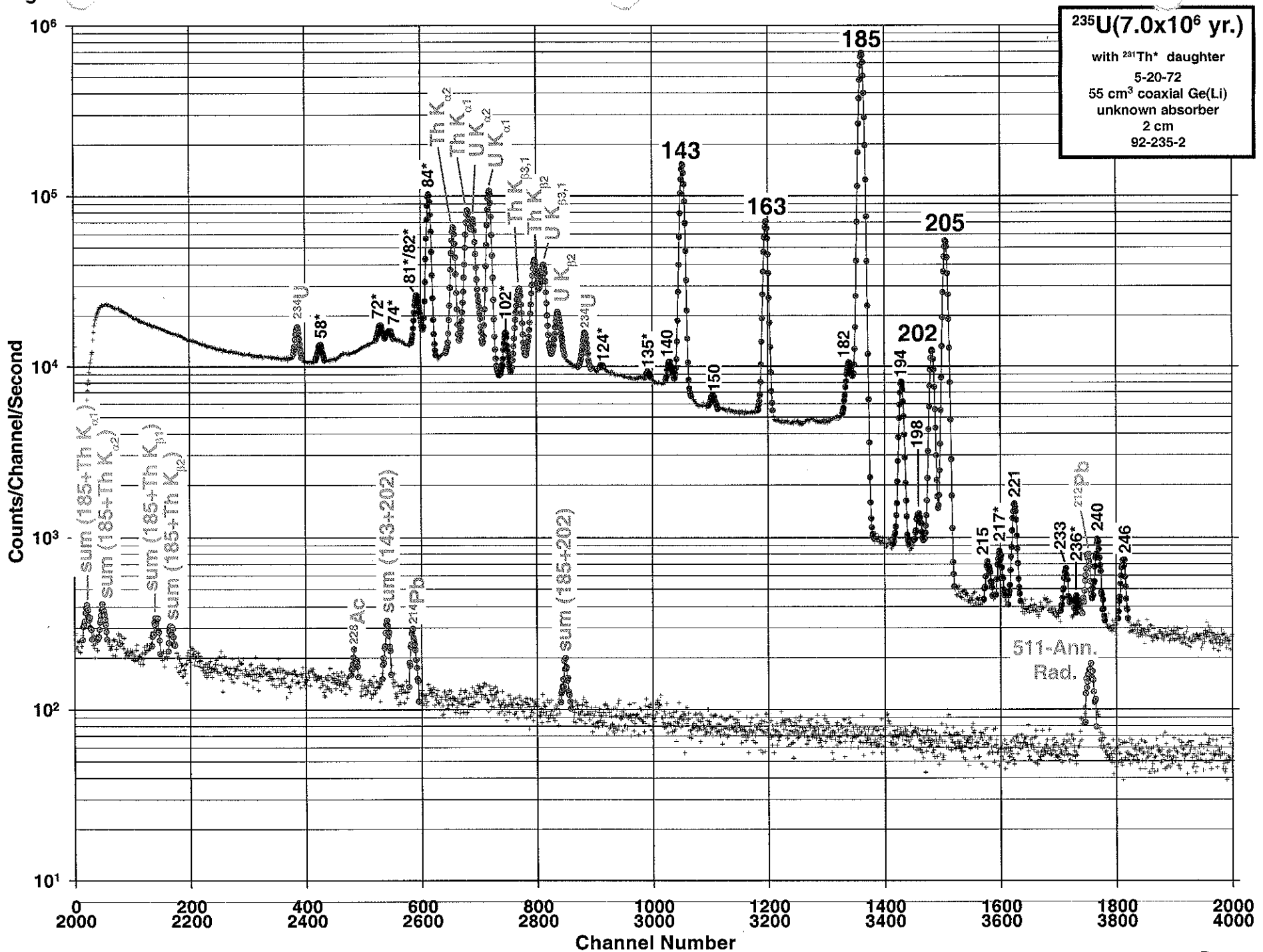

Table of Contents

^{235}U(7.0x10^{6} yr.) Decay Scheme

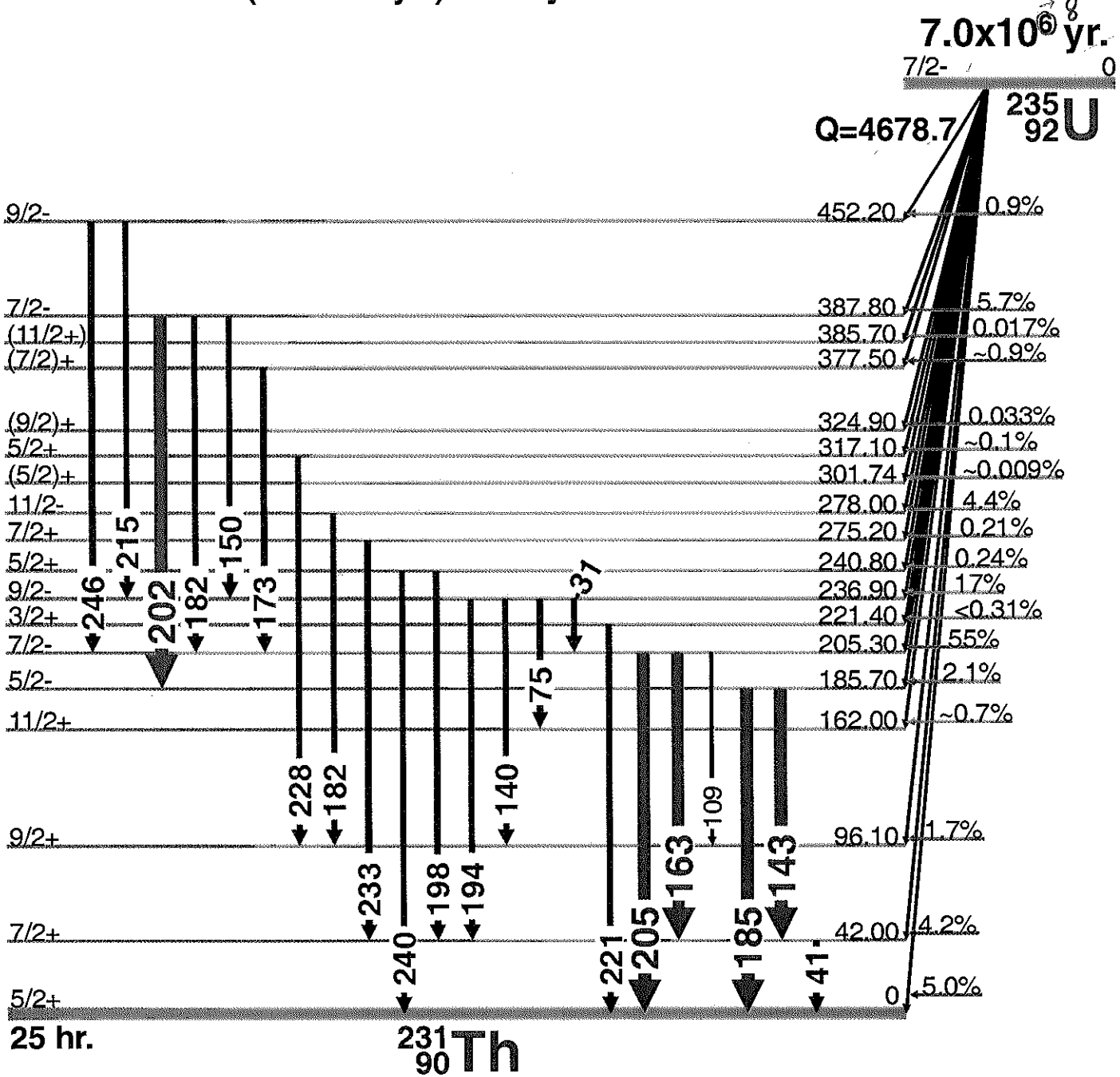

^{235}U Decay Chain

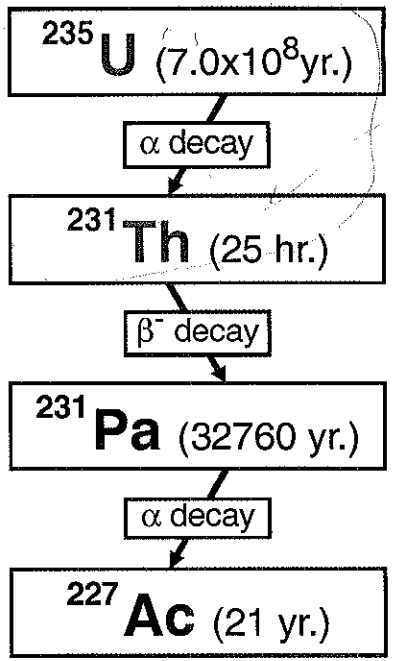

See ^{227}Ac for Chain completion

GAMMA-RAY ENERGIES AND INTENSITIES (page 1 of 2)

Nuclide: ^{235}U

E_γ, σE_γ, I_γ, σI_γ - 1998 ENSDF Data

Half Life: 7.038(5) x10^6 yr.

Detector: 30 mm^2 x 3 mm Si (Li)

Method of Production: U(mass separation)

	E_γ (keV)	σE_γ	I_γ (rel)	I_γ (%)	σI_γ	S
	19.59					4
	31.60	0.05		0.016	0.005	4
^{231}Th	32.73	0.05		0.073	0.004	4
	34.70	0.10		0.0370	0.0004	4
	41.4	0.3		0.030	0.020	4
^{231}Th	41.55	0.05		0.016	0.001	4
	41.96	0.15		0.060	0.010	4
^{231}Th	42.22	0.05		0.052	0.003	4
	51.22	0.10		0.020	0.015	4
	54.10	0.10		0.0020		4
	54.25	0.05		0.0300	0.0003	4
^{231}Th	58.570	0.003		0.48	0.02	3
	60.50					4
	64.370	0.020		0.0400	0.0004	4
	72.70	0.20		0.1100	0.0011	4
^{231}Th	72.751	0.003		0.251	0.015	4
	73.72	0.05		0.0100	0.0001	4
	75.02	0.05	0.25	0.060	0.010	4
^{231}Th	81.228	0.003		0.89	0.05	4
^{231}Th	82.087	0.003		0.40	0.03	4
^{231}Th	84.214	0.003		6.6	0.3	2
^{231}Th	89.95	0.02		0.94	0.06	4
	94.	5.				4
	95.70					4
	96.090	0.020		0.086	0.011	4
^{231}Th	102.270	0.003		0.41	0.03	4
	109.160	0.020	2.77	1.54	0.05	4
	115.45	0.05		0.07	0.04	4
	120.35	0.05		0.0260	0.0003	4
^{231}Th	124.914	0.017		0.056	0.003	4
^{231}Th	135.664	0.011		0.078	0.005	4
	136.55	0.05		0.0120	0.0001	4
	140.76	0.04	0.31	0.220	0.020	4
	142.40	0.05		0.0050	0.0001	4

	E_γ (keV)	σE_γ	I_γ (rel)	I_γ (%)	σI_γ	S
	143.760	0.020	18.0	10.96	0.14	1
	147.00					4
	150.930	0.020	0.20	0.076	0.010	4
^{231}Th	163.101	0.005		0.155	0.009	4
	163.330	0.020	8.52	5.08	0.06	1
	173.3	1.0	0.03	0.010	0.005	4
D	182.10		0.74			4
	182.61	0.05		0.340	0.020	
^{231}Th	183.50	0.02		0.0329	0.013	4
	185.715	0.005	100.	57.2	0.8	1
	194.940	0.010	1.20	0.630	0.012	2
	198.900	0.020	0.05	0.042	0.006	4
	202.110	0.020	1.54	1.080	0.023	1
	205.311	0.010	9.08	5.01	0.07	1
	215.28	0.03	0.05	0.027	0.003	4
^{231}Th	217.94	0.03		0.040	0.03	4
	221.380	0.020	0.22	0.120	0.010	3
	228.78	0.05	0.015	0.008	0.003	4
	233.50	0.03	0.075	0.029	0.005	4
^{231}Th	236.01	0.03		0.0092	0.0006	4
	240.87	0.03	0.14	0.075	0.006	3
	246.84	0.04	0.11	0.053	0.003	3
	251.50	0.10		0.0400	0.0004	4
	266.45	0.05		0.0060	0.0020	4
	275.129			0.042	0.005	4
	275.43	0.10		0.0070	0.0020	4
	279.50	0.05		0.2700	0.0027	4
	281.42	0.05		0.0060	0.0001	4
	282.92	0.05		0.0050	0.0020	4
	289.56	0.04		0.0070	0.0001	4
	291.20					4
	291.65	0.03		0.038	0.005	4
	301.70	0.10		0.0050	0.0001	4

Table of Contents

GAMMA-RAY ENERGIES AND INTENSITIES (page 2 of 2)

Nuclide: ^{235}U E_γ, σE_γ, I_γ, σI_γ - 1998 ENSDF Data Half Life: 7.038(5) x10^6 yr.

Detector: 30 mm^2 x 3 mm Si (Li) Method of Production: U(mass separation)

	E_γ (keV)	σE_γ	I_γ (rel)	I_γ (%)	σI_γ	S
^{231}Th	310.69	0.06		0.0040		4
	311.00	0.05		0.0029	0.0002	4
	317.10	0.08		0.0010		4
	325.80	0.10		0.0004		4
	343.50	0.20		0.0030		4
	345.90	0.03		0.038	0.005	4
	356.03	0.05		0.0050	0.0001	4
	387.82	0.03		0.038	0.005	4

E_γ (keV)	σE_γ	I_γ (rel)	I_γ (%)	σI_γ	S
390.30	0.20		0.040	0.010	4
410.29	0.04		0.0030		4
433.0	0.5		0.0040		4
448.40	0.06		0.0010		4
455.10	0.10		0.0080	0.0001	4
517.2			0.0004		4
742.50	0.20		0.0004		4
794.70	0.10		0.0006		4

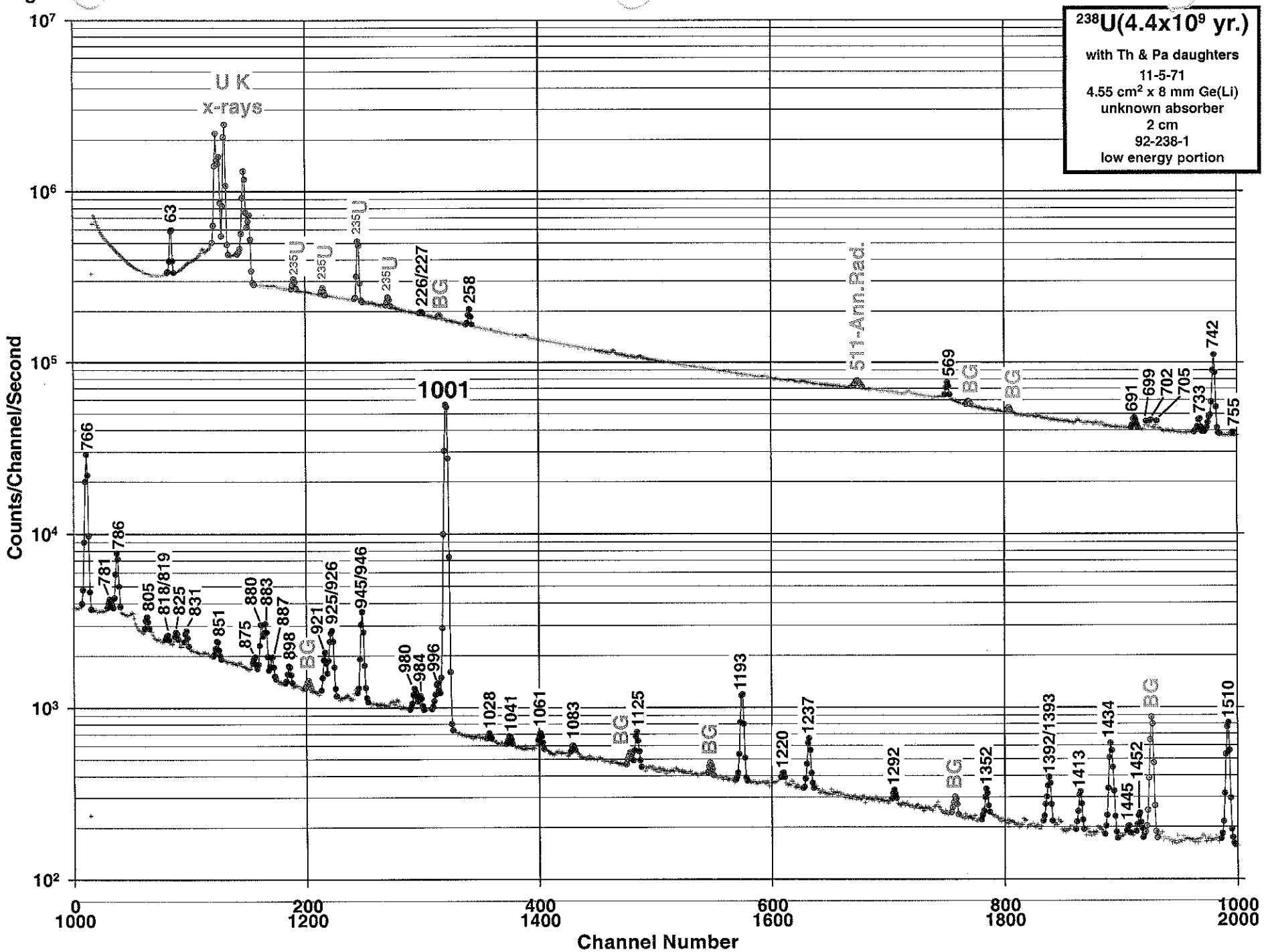

Table of Contents

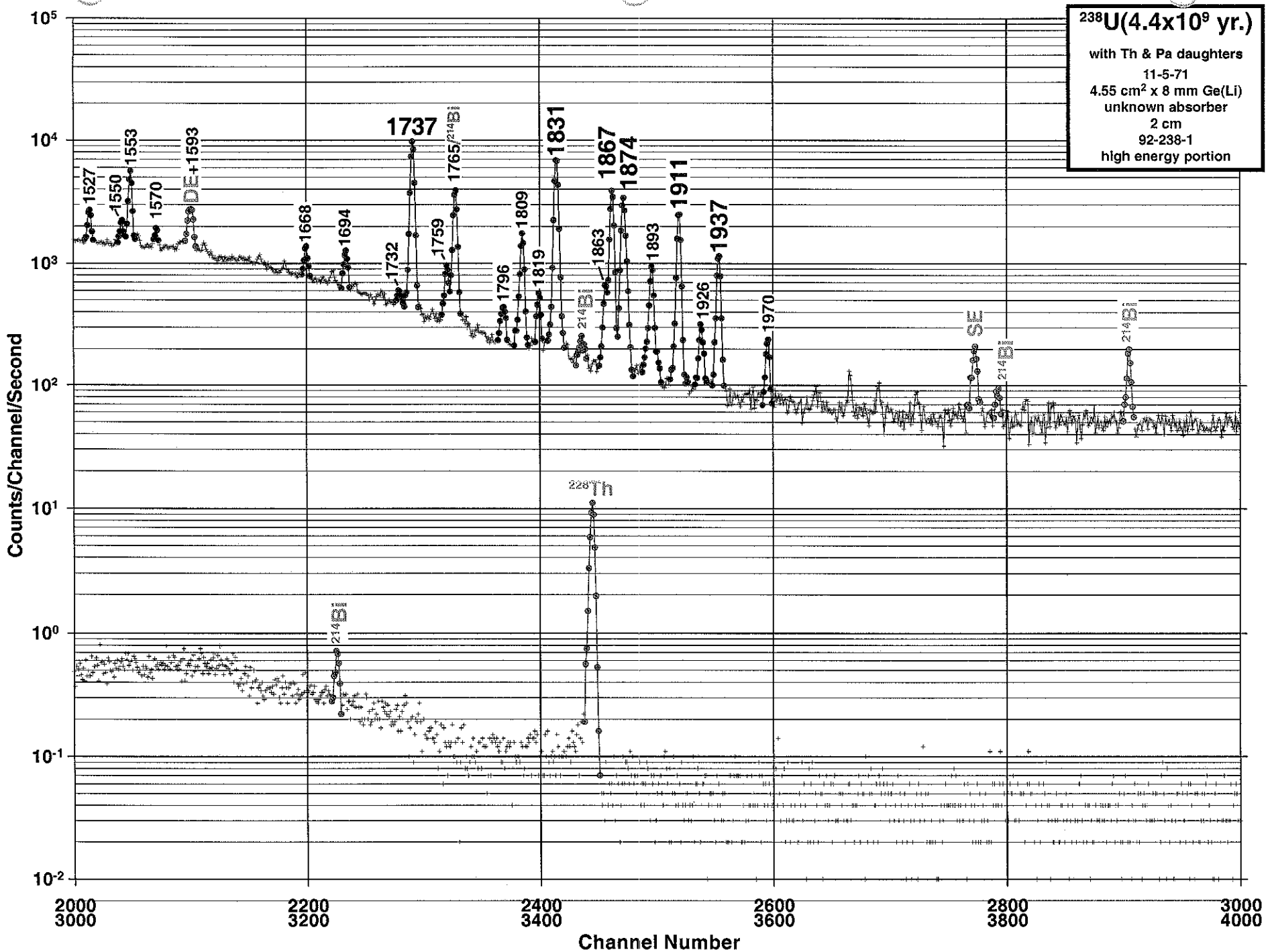

Table of Contents

$^{238}U(4.4x10^{9}$ yr.) Decay Scheme

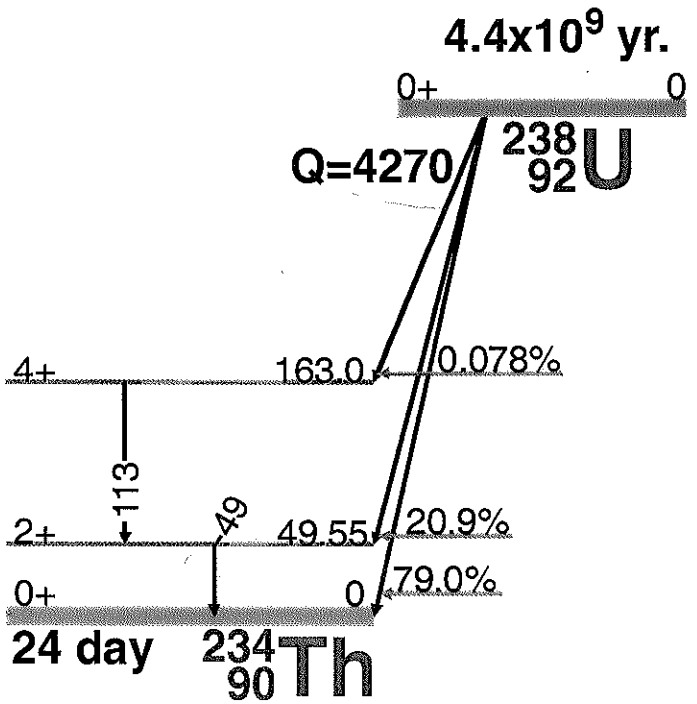

^{238}U Decay Chain

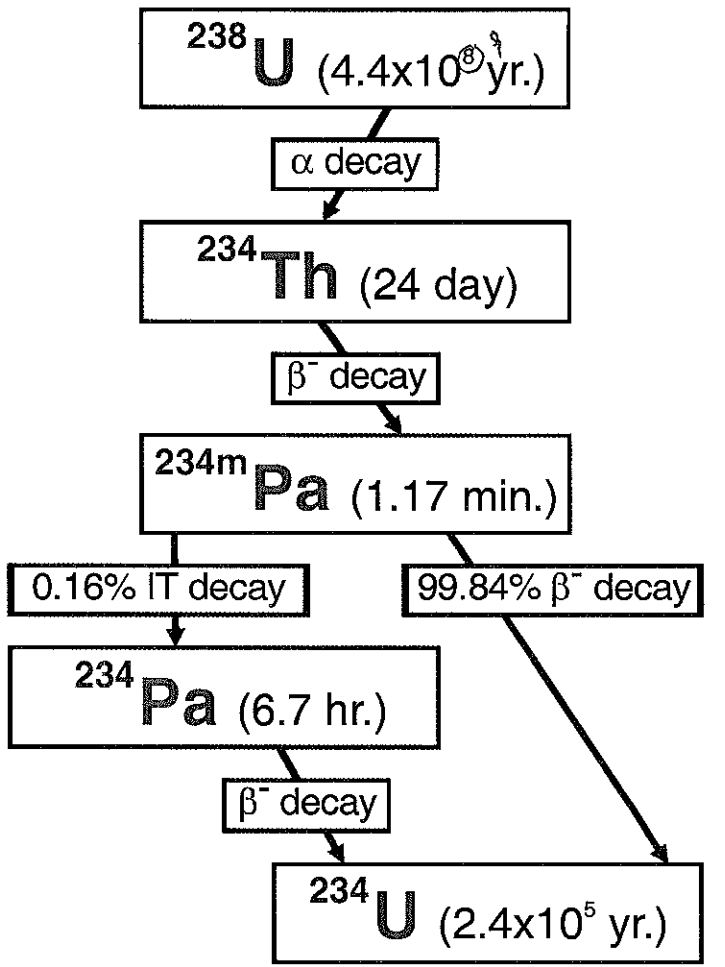

See ^{234}U for Chain completion

GAMMA-RAY ENERGIES AND INTENSITIES (page 1 of 2)

Nuclide: ^{238}U with Th & Pa Daughters
Detector: 4.55 cm^2 x 8 mm Ge (Li)

E_γ, σE_γ, I_γ, σI_γ - 1998 ENSDF Data

Half Life: 4.468(3) x 10^9 yr.
Method of Production: natural U

	E_γ (keV)	σE_γ	I_γ (rel)	I_γ (%)	σI_γ	S
^{238}U	49.55	0.06		0.064	0.008	4
^{234}Th	63.29	0.02		4.8	0.6	3
^{234}Th	92.38	0.01		2.81	0.26	4
^{234}Th	92.80	0.02		2.77	0.26	4
^{238}U	113.5	0.1		0.0102	0.0015	4
^{234}Pa	131.30	0.01	0.433	18.0	1.7	3
^{234}Pa	186.15	0.02	23.3	1.76	0.20	3
^{234}Pa D	226.50	0.03	2.83	4.2	0.5	4
^{234}Pa D	227.25	0.03		5.8	0.6	4
^{234m}Pa	258.26	0.1	3.6	0.0729	0.0004	4
^{234m}Pa D	387.6	0.8	0.06	0.0005		4
^{234m}Pa D	387.6	0.8		0.0010	0.0002	
^{234}Pa	568.9	0.2		3.6	0.5	4
^{234}Pa	569.5	0.1	2.16	8.2	1.1	3
^{234m}Pa	691.0	0.3	1.3	0.0078	0.0007	4
^{234}Pa	699.0	1.0	0.78	0.0008	0.0002	4
^{234}Pa	699.03	0.05		3.6	0.4	
^{234m}Pa	702.05	0.1	0.85	0.0071	0.0002	4
^{234m}Pa	705.90	0.10		0.0040	0.0005	4
^{234}Pa	705.9	0.1		2.27	0.24	
^{234}Pa	733.39	0.05	1.13	6.9	0.8	4
^{234m}Pa	739.95	0.10		0.0117	0.0003	4
^{234m}Pa	742.81	0.03	12.2	0.080	0.004	3
^{234}Pa	742.81	0.03		2.06	0.225	
^{234}Pa	755.0	.01		1.22	0.13	4
^{234m}Pa	766.36	0.02	40	0.294	0.012	2
^{234m}Pa	781.37	0.10	1.17	0.0078	0.0002	4
^{234m}Pa	786.27	0.03	7.17	0.0486	0.0019	3
^{234m}Pa	805.74	0.10	2.3	0.0043	0.0005	4
^{234}Pa	805.8	0.05		2.52	0.29	
^{234m}Pa	818.2	0.5	0.48	0.0010	0.0003	4
^{234}Pa	819.2	0.1		1.88	0.21	

	E_γ (keV)	σE_γ	I_γ (rel)	I_γ (%)	σI_γ	S
^{234}Pa	824.2	0.2		1.24	0.16	
^{234}Pa	825.1	0.2	0.9	1.88	0.21	4
^{234m}Pa	825.6	0.5		0.0014	0.0003	
^{234}Pa	831.5	0.1	1.5	4.1	0.4	4
^{234m}Pa	851.57	0.10	0.95	0.0062	0.0006	4
^{234}Pa	876.0	0.1	0.085	2.52	0.24	4
^{234}Pa	880.5	0.1		4.2	0.4	4
^{234}Pa	880.5	0.1		6.2	0.6	
^{234m}Pa	880.9	0.5	3.17	0.0038	0.0005	3
^{234m}Pa	883.24	0.04		0.0017	0.0005	4
^{234m}Pa	883.24	0.04		0.0018	0.0003	4
^{234}Pa	883.24	0.04	3	9.6	1.1	3
^{234m}Pa	887.28	0.10	1	0.0071	0.0001	4
^{234}Pa	898.67	0.05	1	3.2445	0.3764	4
^{234m}Pa	921.7	0.1	2.16	0.0127	0.0001	4
^{234}Pa D	925.0	0.1	4.3	7.8	0.9	3
^{234}Pa D	926.0	0.2		1.7	1.2	
^{234m}Pa	926.61	0.10		0.0012	0.0001	
^{234}Pa	926.72	0.15		7.2	1.2	
^{234m}Pa	936.3	1	0.13	0.0018	0.0005	4
^{234m}Pa	945.90	0.10	4.5	0.0099	0.0010	3
^{234}Pa	946.00	0.03		3.4	1.5	
^{234}Pa	980.3	0.1	0.67	1.75	0.17	4
^{234}Pa	980.3	0.1		2.68	0.26	
^{234}Pa	984.2	0.1	0.35	1.62	0.22	4
^{234m}Pa	996.1	2.0	1.02	0.0041	0.0007	4
^{234m}Pa	1001.7	0.1		0.838	0.10	1
^{234}Pa	1028.7	0.1	0.25	0.57	0.06	4
^{234m}Pa	1041.7	0.1	0.14	0.0012	0.0001	4
^{234m}Pa	1061.86	0.1	0.48	0.0023	0.0001	4
^{234}Pa	1083.2	0.1	0.15	0.50	0.06	4
^{234m}Pa	1125.7	0.5	0.3	0.0035	0.0006	4

NOTE: ^{234}Pa - multiply I_γ(%) values by 0.0016 to account for branching from ^{234m}Pa

Table of Contents

GAMMA-RAY ENERGIES AND INTENSITIES (page 2 of 2)

Nuclide: ^{238}U with Th & Pa Daughters
Detector: 4.55 cm^2 x 8 mm Ge (Li)

E_γ, σE_γ, I_γ, σI_γ - 1998 ENSDF Data

Half Life: 4.468(3) x 10^9 yr.
Method of Production: natural U

	E_γ (keV)	σE_γ	I_γ (rel)	I_γ (%)	σI_γ	S
^{234}Pa	1151.4	0.3	0.03	0.031	0.010	4
^{234m}Pa	1193.77	0.03	1.65	0.0135	0.0001	3
^{234m}Pa	1220.37	0.10	0.14	0.0009	0.0001	4
	1226.4	0.2	0.08		0.03	4
^{234m}Pa	1237.24	0.10	0.62	0.0053	0.0001	3
^{234}Pa	1292.8	0.1	0.07	0.46	0.05	4
^{234}Pa	1352.9	0.1	0.15	1.15	0.12	4
^{234m}Pa	1392.7	1.0		0.0034	0.0002	3
^{234}Pa	1393.9	0.1	0.48	2.06	0.22	3
^{234}Pa	1400.3	0.1	0.08	0.175	0.026	4
^{234m}Pa	1413.88	0.10	0.32	0.0023	0.0001	4
^{234}Pa	1426.9	0.1	0.05	0.164	0.026	4
^{234m}Pa	1434.13	0.10	1.2	0.0097	0.0001	3
^{234}Pa	1445.4	0.1	0.06	0.31	0.04	4
^{234}Pa	1452.7	0.1	0.12	0.80	0.09	4
^{234m}Pa	1510.2	0.1	1.6	0.0129	0.0002	2
^{234m}Pa	1527.27	0.10	0.28	0.0024	0.0001	3
^{234m}Pa	1550.0	1.0	0.2	0.0018	0.0002	4
^{234m}Pa	1553.74	0.10	1	0.0081	0.0001	3
^{234m}Pa	1570.67	0.10		0.0011	0.0001	4
^{234m}Pa	1593.88	0.10		0.0027	0.0001	4
^{234m}Pa	1667.6	1.0		0.0008	0.0002	4

	E_γ (keV)	σE_γ	I_γ (rel)	I_γ (%)	σI_γ	S
^{234}Pa	1668.4	0.1	0.18	0.76	0.09	3
^{234}Pa	1685.7	0.1	0.07	0.31	0.04	4
^{234m}Pa	1694.1	1.0	1.8	0.0005	0.0001	3
^{234m}Pa	1732.2	1.5		0.0018	0.0003	4
^{234m}Pa	1737.73	0.1		0.0211	0.0003	1
^{234m}Pa	1759.81	0.10	0.2	0.0014	0.0007	3
^{234m}Pa	1765.44	0.10	1	0.0087	0.0001	2
^{234m}Pa	1796.2	1	0.09	0.0003	0.0001	3
^{234m}Pa	1809.04	0.10	0.45	0.0037	0.0001	2
^{234m}Pa	1819.69	0.10		0.0009	0.0001	3
^{234}Pa	1819.8	0.3	0.1	0.0041	0.0011	3
^{234m}Pa	1831.3	0.1	2.2	0.0172	0.0003	1
^{234}Pa	1849.8	0.2	0.01	0.0278	0.0067	4
^{234m}Pa	1863.09	0.10	0.18	0.0012	0.0001	3
^{234m}Pa	1867.68	0.10	1.2	0.0092	0.0001	1
^{234m}Pa	1874.85	0.10	1.2	0.0082	0.0001	1
^{234m}Pa	1893.5	0.1	0.35	0.0022	0.0001	2
^{234m}Pa	1911.17	0.10	0.77	0.0063	0.0001	1
^{234m}Pa	1926.5	1.0	0.08	0.0004	0.0001	3
^{234m}Pa	1937.01	0.10	0.35	0.0029	0.0001	1
^{234m}Pa	1970.0	1.5	0.045	0.0006	0.0001	3

NOTE: ^{234}Pa - multiply I_γ(%) values by 0.0016 to account for branching from ^{234m}Pa

Table of Contents

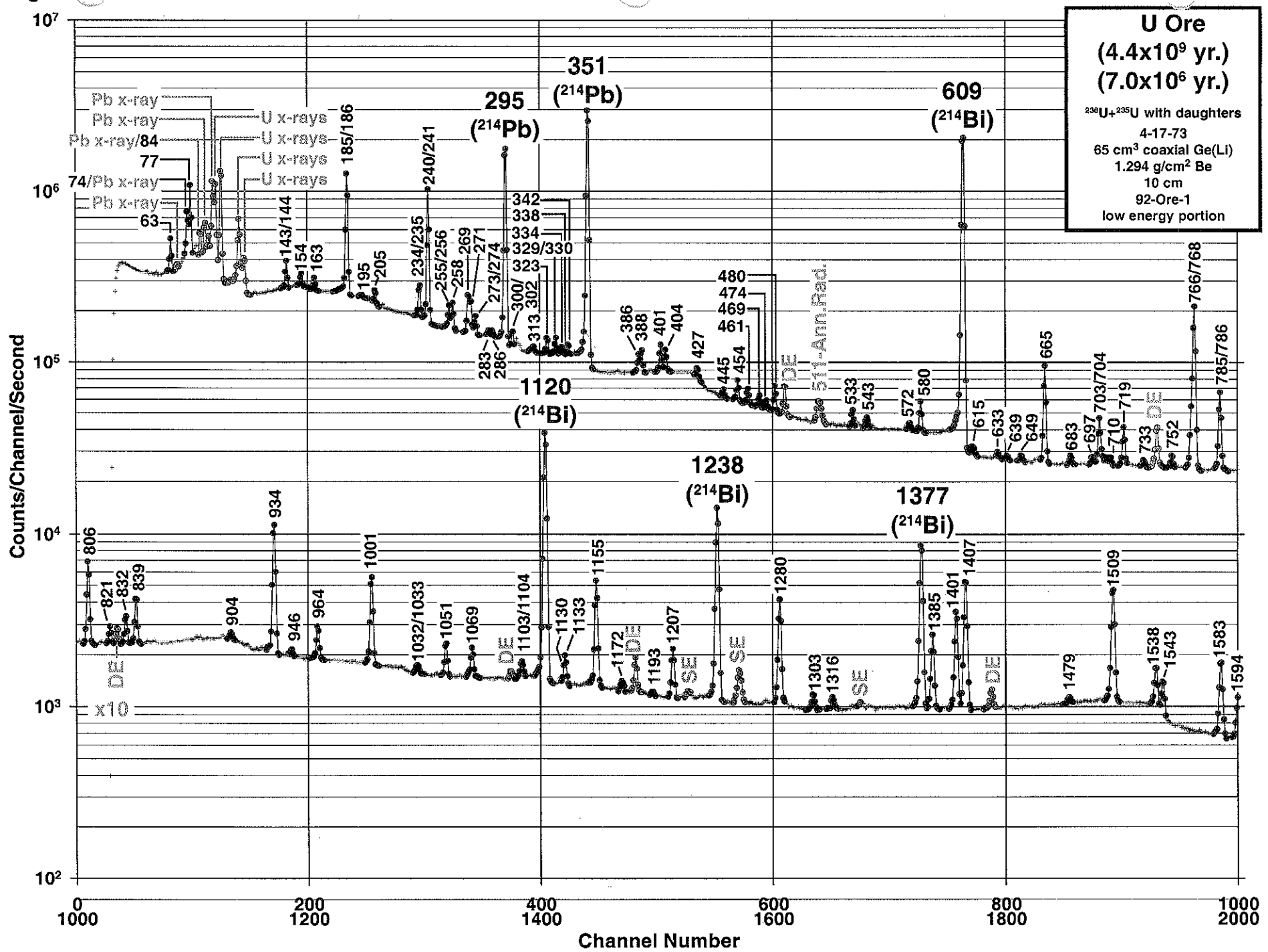

Table of Contents

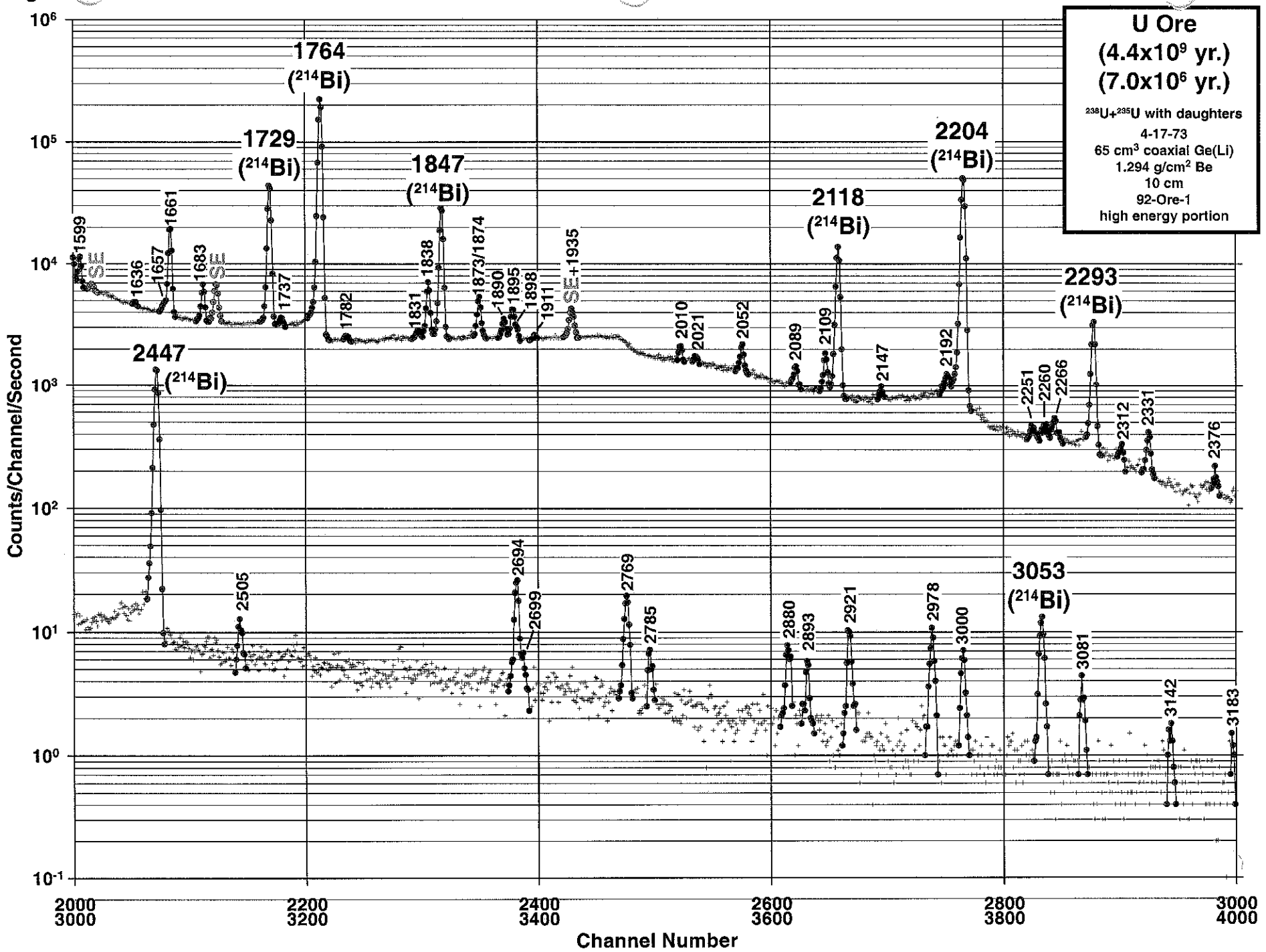

Table of Contents

^{235}U Decay Chain

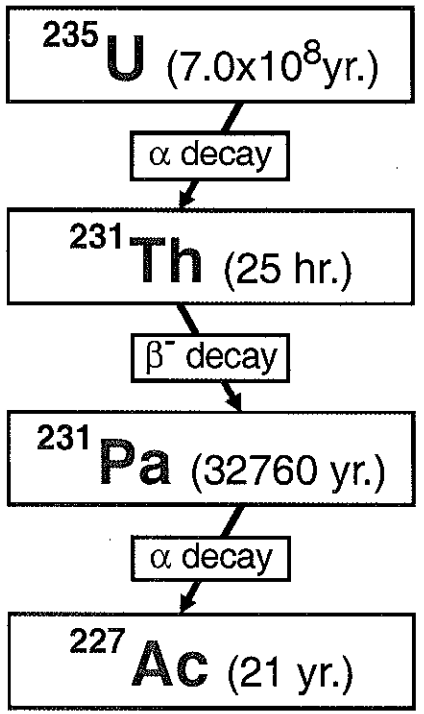

See ^{227}Ac for Chain completion

^{238}U Decay Chain

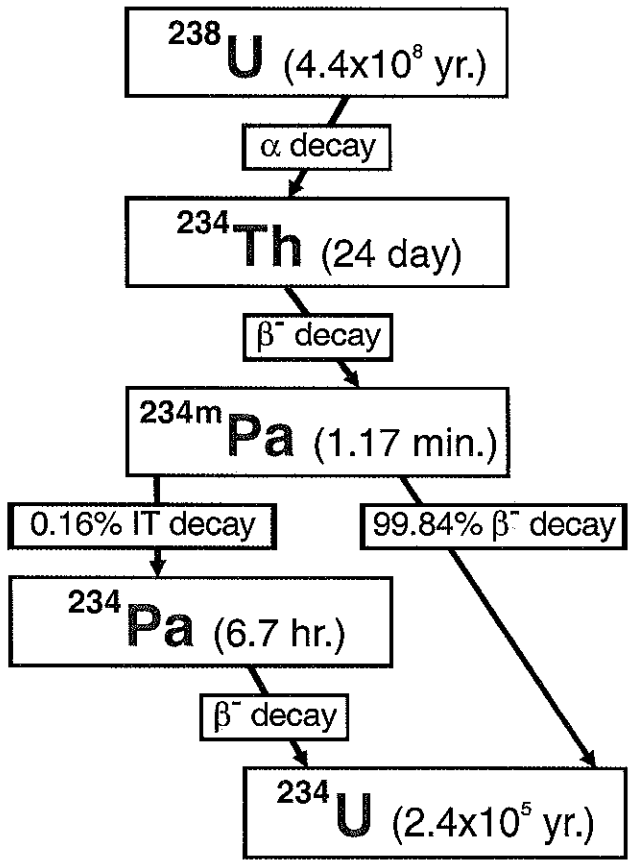

See ^{234}U for Chain completion

GAMMA-RAY ENERGIES AND INTENSITIES (page 1 of 2)

Nuclide: Uranium Ore (^{238}U + ^{235}U with daughters)

Half Life: 4.468(3) x 10^9 yr. + 7.038(5) x 10^6 yr.

E_γ, σE_γ - 1998 ENSDF Data For I_γ, σI_γ - 1998 ENSDF Data, See: ^{226}Ra, ^{235}U, and ^{238}U Spectra

Detector: 65 cm^3 coaxial Ge (Li)

Method of Production: Natural Radioactivity

Isotope	E_γ (keV)	σE_γ	S
^{234}Th	63.29	0.02	4
^{231}Pa	63.65	0.02	
^{231}Pa	74.15	0.04	4
^{231}Pa	77.34	0.03	3
^{231}Th	84.214	0.003	4
^{234}Th	92.38	0.01	3
^{234}Th	92.80	0.02	
^{235}U	143.76	0.02	4
^{223}Ra	144.23	0.01	
^{223}Ra	154.21	0.01	4
^{235}U	163.33	0.02	4
^{235}U	185.715	0.005	2
^{226}Ra	186.211	0.013	
	195.70	0.20	4
^{235}U	205.311	0.010	4
^{223}Fr	234.80	0.01	4
^{234m}Pa	235.85	0.18	
^{227}Th	235.971	0.020	
^{224}Ra	240.986	0.006	2
^{214}Pb	241.977	0.003	
^{231}Pa	255.77	0.05	4
^{227}Th	256.25	0.02	
^{214}Pb	258.87	0.20	4
^{228}Ac	269.28	0.04	4
^{223}Ra	269.459	0.010	
^{219}Rn	271.23	0.01	4
^{231}Pa	273.14	0.06	4
^{214}Bi	273.80	0.5	
^{214}Pb	274.80	0.05	
^{231}Pa	283.69	0.01	4
^{227}Th	286.122	0.020	4
^{214}Pb	295.224	0.002	1
^{227}Th	300.00	0.03	4
^{231}Pa	302.65	0.01	
^{227}Th	314.78	0.09	4
^{223}Ra	323.87	0.01	4
^{227}Th	329.851	0.02	4
^{231}Pa	330.06	0.01	

Isotope	E_γ (keV)	σE_γ	S
^{227}Th	334.38	0.02	4
^{223}Ra	338.281	0.010	4
^{228}Ac	338.32	0.06	
^{227}Th	342.50	0.09	4
^{211}Bi	351.06	0.04	1
^{214}Bi	351.9	0.5	
^{214}Pb	351.932	0.002	
^{214}Bi	386.77	0.05	4
^{214}Bi	388.88	0.05	4
^{219}Rn	401.81	0.01	4
^{211}Pb	404.853	0.010	4
^{214}Bi	405.74	0.3	
^{211}Pb	427.088	0.010	4
^{223}Ra	445.03	0.01	4
^{214}Bi	454.77	0.12	4
^{214}Bi	461.00	0.2	4
^{214}Bi	469.76	0.07	4
^{214}Bi	474.41	0.05	4
^{214}Pb	480.43	0.08	4
^{214}Pb	533.66	0.02	4
^{214}Bi	543.0	0.2	4
^{214}Bi	572.76	0.07	4
^{214}Pb	580.13	0.03	4
^{214}Bi	609.312	0.007	1
^{214}Bi	615.73	0.10	4
^{214}Bi	633.14	0.10	4
^{214}Bi	639.67	0.10	4
^{214}Bi	649.18	0.07	4
^{214}Bi	665.453	0.022	3
^{214}Bi	683.22	0.06	4
^{214}Bi	697.90	0.25	4
^{214}Bi	703.11	0.04	4
^{211}Pb	704.64	0.03	
^{214}Bi	710.67	0.10	4
^{214}Bi	719.86	0.03	4
^{214}Bi	733.80	0.15	4

Isotope	E_γ (keV)	σE_γ	S
^{214}Bi	752.84	0.03	4
^{234m}Pa	766.36	0.02	2
^{234m}Pa	766.51	0.03	
^{211}Pb	766.63	0.15	
^{214}Bi	768.356	0.010	
^{214}Pb	785.96	0.09	3
^{214}Bi	786.1	0.4	
^{234m}Pa	786.27	0.03	
^{214}Bi	806.174	0.018	3
^{214}Bi	821.18	0.03	4
^{211}Pb	832.01	0.03	4
	839.05	0.06	4
^{214}Bi	904.29	0.10	4
^{214}Bi	934.061	0.012	4
	946.04	0.10	4
^{214}Bi	964.08	0.03	4
^{234m}Pa	1001.7	0.1	3
^{214}Bi	1032.37	0.08	4
^{214}Bi	1033.3	0.2	
^{214}Bi	1051.96	0.03	4
^{214}Bi	1069.96	0.08	4
^{214}Bi	1103.64	0.19	4
^{214}Bi	1104.79	0.19	
^{214}Bi	1120.287	0.010	1
^{214}Bi	1130.29	0.19	4
^{214}Bi	1133.66	0.03	4
^{214}Bi	1155.19	0.02	3
^{214}Bi	1172.98	0.10	4
^{234m}Pa	1193.77	0.003	4
^{214}Bi	1207.68	0.03	4
^{214}Bi	1238.110	0.012	1
^{214}Bi	1280.96	0.02	3
^{214}Bi	1303.76	0.08	4
^{214}Bi	1316.96	0.15	4
^{214}Bi	1377.669	0.012	1
^{214}Bi	1385.31	0.03	3
^{214}Bi	1401.50	0.05	3

Table of Contents

GAMMA-RAY ENERGIES AND INTENSITIES (page 2 of 2)

Nuclide: Uranium Ore (^{238}U + ^{235}U with daughters)

Half Life: 4.468(3) x 10^9 yr. + 7.038(5) x 10^6 yr.

E_γ, σE_γ - 1998 ENSDF Data For I_γ, σI_γ - 1998 ENSDF Data, See: ^{226}Ra, ^{235}U, and ^{238}U Spectra

Detector: 65 cm^3 coaxial Ge (Li)

Method of Production: Natural Radioactivity

Isotope	E_γ (keV)	σE_γ	S
^{214}Bi	1385.31	0.03	3
^{214}Bi	1401.50	0.05	3
^{214}Bi	1407.98	0.04	2
^{214}Bi	1479.15	0.14	4
^{214}Bi	1509.228	0.015	3
^{214}Bi	1538.50	0.06	4
^{214}Bi+sum(734+609)	1543.32	0.06	4
^{214}Bi	1583.22	0.04	3
^{214}Bi	1594.73	0.08	4
^{214}Bi	1599.31	0.06	4
^{214}Bi	1636.3	0.2	4
^{214}Bi	1657.00	0.19	4
^{214}Bi	1661.28	0.06	2
^{214}Bi	1683.99	0.04	3
^{214}Bi	1729.595	0.015	1
^{234m}Pa	1737.73	0.01	4
^{214}Bi	1764.494	0.014	1
	1782.3	0.4	4
^{234m}Pa	1831.3	0.1	4
^{214}Bi	1838.36	0.05	3

Isotope	E_γ (keV)	σE_γ	S
^{214}Bi+sum(609+1238)	1847.420	0.025	1
^{214}Bi	1873.16	0.06	3
^{234m}Pa	1874.85	0.10	
^{214}Bi	1890.30	0.15	4
^{214}Bi	1895.92	0.14	4
^{214}Bi	1898.7	0.4	4
^{234m}Pa	1911.17	0.10	4
^{214}Bi	1935.5	0.2	4
^{214}Bi	2010.78	0.12	4
^{214}Bi	2021.6	0.2	4
^{214}Bi	2052.94	0.12	4
^{214}Bi	2089.70	0.20	4
^{214}Bi	2109.92	0.12	4
^{214}Bi	2118.55	0.03	1
^{214}Bi	2147.9	0.2	4
^{214}Bi	2192.58	0.16	4
^{214}Bi	2204.21	0.04	1
^{214}Bi	2251.6	0.2	4
^{214}Bi	2260.3	0.2	4

Isotope	E_γ (keV)	σE_γ	S
^{214}Bi	2266.51	0.13	4
^{214}Bi	2293.40	0.12	1
^{214}Bi	2312.4	0.2	4
^{214}Bi	2331.3	0.2	4
^{214}Bi	2376.9	0.2	4
^{214}Bi	2447.86	0.10	1
^{214}Bi	2505.4	0.2	4
^{214}Bi	2694.7	0.2	2
^{214}Bi	2699.4	0.3	4
^{214}Bi	2769.9	0. 2	2
^{214}Bi	2785.9	0.2	3
^{214}Bi	2880.3	0.2	3
^{214}Bi	2893.5	0.2	3
^{214}Bi	2921.9	0.2	2
^{214}Bi	2978.9	0.2	2
^{214}Bi	3000.0	0.2	2
^{214}Bi	3053.9	0.2	1
^{214}Bi	3081.7	0.3	2
^{214}Bi	3142.6	0.4	4
^{214}Bi	3183.6	0.4	4

Table of Contents

EXPERIMENT 7

High-Resolution Gamma-Ray Spectroscopy

EQUIPMENT NEEDED FROM EG&G ORTEC

Source Kit SK-1G
Other sources: 5 μCi of ^{137}Cs; 10 μCi of ^{60}Co; 10 μCi of ^{228}Th
Bin and Power Supply
GEM-10195 Coaxial Detector System (includes detector, cryostat, dewar, and preamplifier); typical specifications, 10% efficiency, 1.95-keV resolution at 1.33 MeV, 37:1 peak-to-Compton
459 5 kV Detector Bias Supply
572 Spectroscopy Amplifier
444 Gated Biased Amplifier
480 Pulser
ACE-2K MCA System including suitable IBM PC (other EG&G ORTEC MCAs may be used)
Oscilloscope
(Optional for Experiment 7.4) a 1- to 3-Ci americium-beryllium isotopic neutron source; if the source is not in a paraffin howitzer, place a 6-in. thickness of paraffin between the source and the HPGe detector to thermalize the source neutrons.
ORC-7 Cable Set

Purpose

Gamma-ray energies will be measured with a high-purity germanium (HPGe) detector and research-grade electronics. The theory of response characteristics is explained, and the high-resolution results of measurement are contrasted with an NaI(Tl) scintillation detector in Experiment 3.

Introduction

Most of the experiments in this manual are written for use with EG&G ORTEC educational modules. In this experiment, which illustrates the high-resolution capabilities of HPGe detector systems, research-grade modules have been listed in order to process the pulses from the HPGe detector with a greater degree of precision to complement the detector capabilities.

Many colleges, both large and small, have Nuclear Spectroscopy Centers. In these laboratories the research efforts of the department will normally be directed in the area of high-resolution gamma-ray spectroscopy. It is possible to do a great amount of publishable research on such work as decay scheme analysis, etc., with these high-resolution systems. In many cases additional lines can be found in spectra or the improved resolution can reveal a doublet, whereas earlier measurements with NaI(Tl) detectors indicated a single energy line.

The latest decay schemes for isotopes are included in refs. 10 and 12. More recent information on certain nuclei can be obtained by writing

The Nuclear Data Project
Building 4500
Oak Ridge National Laboratory
Post Office Box X
Oak Ridge, Tennessee 37831 U.S.A.

In Experiment 3 gamma spectroscopy was studied with NaI(Tl) detectors. Typical energy resolution that can be obtained with NaI(Tl) is ~7% for the 0.661-MeV ^{137}Cs gamma line. For NaI(Tl) detectors the resolution is a strong function of energy. Variation of resolution results primarily from the statistical fluctuation of the number of photoelectrons that are produced at the photocathode surface in the photomultiplier tube. Table 7.1 illustrates some typical resolutions for NaI(Tl) spectroscopy as functions of the gamma energies.

The use of germanium detectors has completely revolutionized gamma spectroscopy. Figure 7.1 illustrates the striking contrast of results obtained with these two types of

Table 7.1. Typical Resolutions of NaI(Tl) for Different Gamma Energies.

Isotope	Gamma Energy (keV)	Resolution (%)
^{166}Ho	81	16.19
^{177}Lu	113	13.5
^{133}Te	159	11.5
^{177}Lu	208	10.9
^{203}Hg	279	10.14
^{51}Cr	320	9.89
^{198}Au	411	9.21
^{7}Be	478	8.62
^{137}Cs	661	7.7
^{54}Mn	835	7.26
^{207}Bi	1067	6.56
^{65}Zn	1114	6.29
^{22}Na	1277	6.07
^{88}Y	1850	5.45

The information for this table was taken from *IRE Trans. Nucl. Sci.* **NS-3**(4), 57 (Nov. 1956). "Intrinsic Scintillator Resolution," by G. G. Kelley *et al.*, quoting results from F. K. McGowan, *et al.*

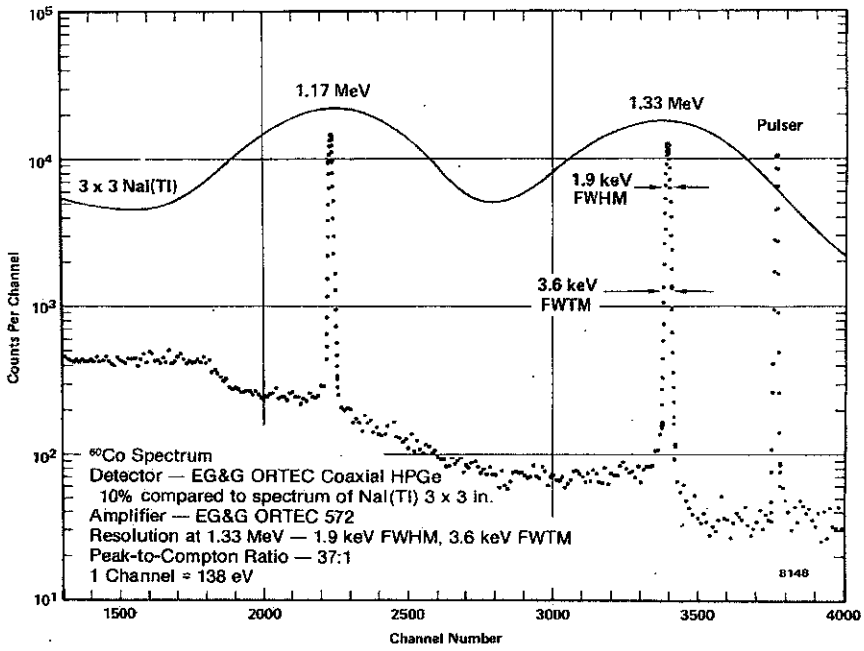

Fig. 7.1. ^{60}Co Spectrum Showing Resolutions and Peak-to-Compton Ratios for an HPGe Coaxial Detector and an NaI(Tl) Detector.

detectors. There is a factor of 30 improvement of the resolution of the data at the full-width at half-maximum (FWHM) count levels. As a result of the improved resolution, many nuclear energy levels that could not even be seen with NaI(Tl) detectors are identified easily with HPGe detectors.

In a parallel fashion the development of Si(Li) detectors has revolutionized x-ray spectroscopy. These Si(Li) devices will be studied in Experiment 8.

The purpose of this experiment is to study some of the properties of the HPGe detector systems. This experiment deals only with the practical aspects of making measurements with these detectors. To understand the properties of these detection systems, the following brief review of gamma-ray interactions and pair-production processes is included.

In Experiment 3 it was pointed out that the pair-production process at gamma energies >3 MeV is a very important gamma interaction. Figure 7.2 shows graphs for the three important gamma interactions for both germanium and silicon. The information for germanium is of interest in this experiment, and that for silicon will be used in Experiment 8.

When a gamma enters a detector, it must produce a recoil electron by one of three processes before it is recorded as an event: the photoelectric effect, the Compton effect, or pair production.

In the photoelectric process the gamma or x ray gives all of its energy to the recoil electron. It is the recoil electron that produces the electron-hole pairs in the detector that yield the output pulse. For the photoelectric process the output pulse from the detector is proportional to the energy of the

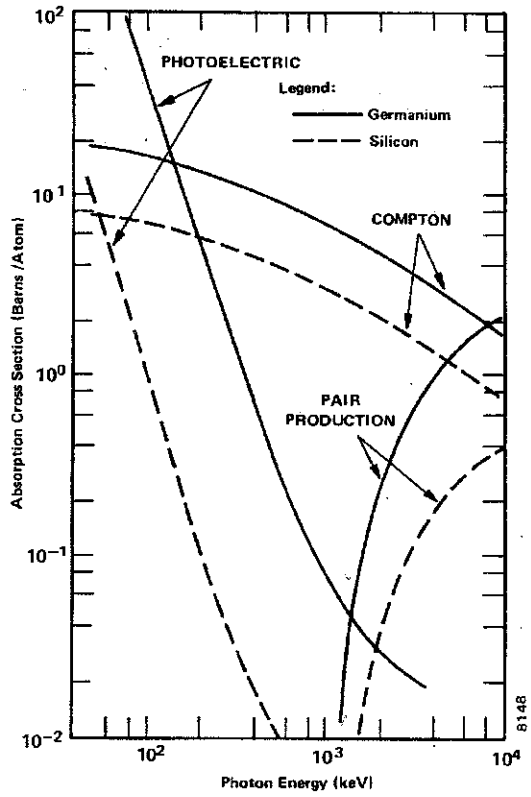

Fig. 7.2. Relative Probability of Each of the Three Types of Interactions as a Function of Energy.

gamma or x ray that produced the interaction. In the spectrum these events will show up as full-energy photopeaks.

In the Compton process there is a distribution of pulse amplitudes up to some maximum pulse height. This maximum pulse height produces the Compton edge, as explained in Experiment 3, and there is a statistical probability that each event can produce a pulse with any height up to this maximum with about an equal chance. Thus Compton events will provide a well-distributed low-energy area in the spectrum.

In modern, large detectors with high peak-to-Compton ratios, some Compton events also contribute to the full energy peak when the scattered photons undergo one or more additional interactions. This results in complete absorption.

The pair-production process can also provide a total absorption of the gamma-ray energy. The gamma enters the detector and creates an electron-positron pair. From the law of conservation of mass and energy it follows that the initial gamma must have an energy of at least 1.02 MeV because it takes that much energy to create both the negative and positive electrons. The net mass that is produced is two electron masses, and this satisfies the law of conservation of energy, $E = mc^2$.

Note that 1.02 MeV is about twice the annihilation energy that was measured from ^{22}Na (0.511 MeV). Figure 7.3 illustrates what happens in the detector in the pair-production process.

In Fig. 7.3 the e (ordinary electron) will produce a pulse whose magnitude is proportional to the energy of e^- (E_{e^-}). The positron will produce a pulse proportional to E_{e^+}. Since these two pulses are produced simultaneously, the output pulse from the detector would be the sum of the two pulses. When the positron annihilates in the detector, the annihilation radiation, γ_1 and γ_2, will be produced. In Fig. 7.3 both γ_1 and γ_2 are shown escaping from the boundaries of the detector without making any further interactions. (Note: $\gamma_1 = \gamma_2 = 0.511$ MeV.) Thus, for this example, an energy of exactly 1.02 MeV escapes from the detector and is subtracted from the total energy that entered the detector. It is possible for only one, either γ_1 or γ_2, to make a photoelectric interaction in the detector while the other escapes. In such cases the total energy absorbed is 0.511 MeV less than the original incident gamma energy. It is also possible for both

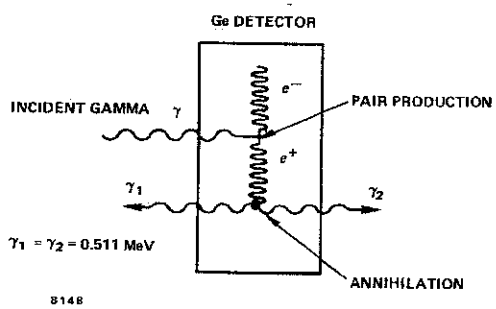

Fig. 7.3. Process of Pair Production in Germanium.

gammas to make photoelectric interactions without escaping, with all the original energy then being left in the detector. Therefore in the spectrum that is measured there will be three peaks for each gamma energy. These peaks are labeled Full-Energy Peak, Single-Escape Peak, and Double-Escape Peak, and they will be separated by 0.511-MeV increments. Figure 7.4 shows a typical spectrum that would be obtained for an incident gamma energy of 2.511 MeV. The lower end of the spectrum that includes the Compton distribution has not been included; this effect is obtained by using a biased amplifier to eliminate the lower energies and to expand the distribution of the higher-energy pulses across the range that is measured. The Single-Escape Peak occurs at (E_γ – 0.511 MeV) or 2.00 MeV, and the Double-Escape Peak occurs at (E_γ – 1.02 MeV) or 1.49 MeV. Of course, the full-energy peak represents those events for which there was a combination of pair production and photoelectric effect in which all the energy was absorbed in the detector.

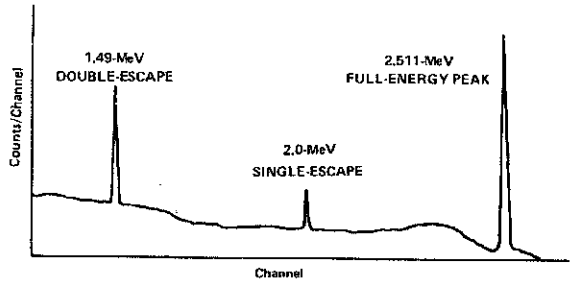

Fig. 7.4. Typical Spectrum for an Incident Gamma Energy of 2.511 MeV.

Now refer again to Fig. 7.2 and specifically to the curves for the interactions in germanium. The absorption cross section, plotted in the y direction, is a measure of the relative probability that an interaction will take place in a germanium detector. These probabilities of relative interactions, for the most part, determine the shape of the observed spectrum. For example, a photon (or gamma) with an energy of 100 keV has an absorption cross section of ~55 barns/atom for the photoelectric process. The corresponding Compton cross section is ~18 barns/atom. There is no pair production. This indicates that at 100 keV there are 3 times as many photoelectric interactions as Compton interactions, since this is the approximate ratio of the cross section. Figure 7.5 shows the shape of a spectrum that could be expected for measurement of the 100-keV energy events.

The sum of counts under the photopeak would be 3 times the sum under the Compton distribution. For larger crystals Σ_{pp} would be even >3 times Σ_c because some of the scattered gammas from the Compton interactions would make photoelectric interactions before escaping from the crystal. For an infinitely large crystal there would be no Compton distribution since the crystal would then totally absorb all of the incident gammas.

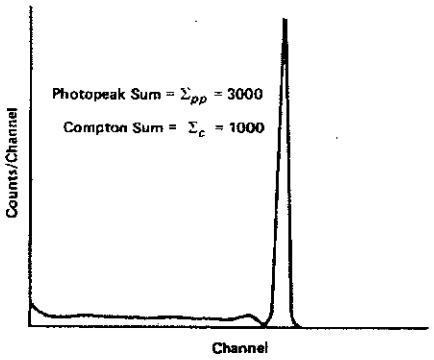

Fig. 7.5. Typical Spectrum Expected for 100-keV Energy in HPGe.

The shape of the spectrum changes drastically from 100 keV to 1 MeV. Figure 7.6 shows the gamma spectrum that could be expected for the 1-MeV gammas incident on an HPGe detector. From Fig. 7.2 the ratio of Compton cross section to photoelectric cross section is ~90; so in Fig. 7.6, Σ_c is 90,000 and Σ_{pp} is 1000. The variation of cross sections for HPGe and Si(Li) detectors can also be approximated from Fig. 7.2. For example, at E_γ = 400 keV the photoelectric cross section for germanium is 6 barns/atom and that for silicon is ~0.1 barn/atom. This is a ratio of 60:1 and indicates that there will be 60 times as many counts under the photopeak for a germanium detector as for a silicon detector at 400 keV, assuming that the detectors are the same size. The reason for this is that the photoelectric cross section varies as Z^5, where Z is the atomic number of the absorbing material. The atomic number of Ge is 32 and is 14 for Si. The ratio of these two numbers raised to the 5th power is 62.22, and this is within remarkable agreement with the above cross-section ratios.

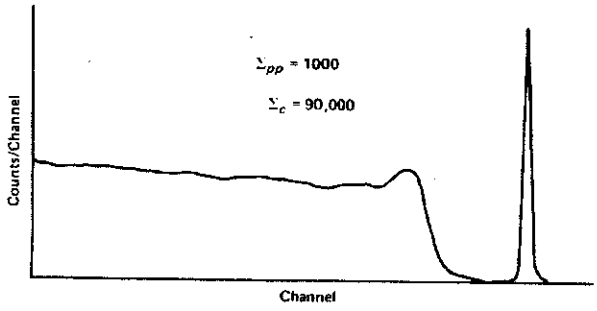

Fig. 7.6. Typical Spectrum Expected for 1-MeV Energy in HPGe.

EXPERIMENT 7.1

Energy Resolution with an HPGe Detector

The instructor will provide the HPGe detector and the instructions for its use. Read the instruction manual carefully before attempting to use the detector. This is a very expensive detector system and must be handled carefully.

Procedure

1. Install the 459, 480, 572, and 444 in the bin and power supply and interconnect the modules as shown in Fig. 7.7. The preamplifier will be mounted on the HPGe detector and the interconnection for the signal connections to the detector is made through the preamplifier. Connect the 459 to the Detector Bias Input and connect the 480 to the Test Input on the preamplifier. Connect the power cable for the preamplifier to the Preamplifier Power connector on the 572. Connect a signal output from the preamplifier to the 572 input. Connect the Unipolar Out from the 572 to the linear input of the 444, and connect the 444 output to the input of the MCA. Set the module controls as follows:

572 Amplifier: Positive input (verify with instructor); Unipolar Output; Shaping time 6 μs; Delay Out.

444 Gated Biased Amplifier: Coarse Gain X2; Fine Gain 1/2; Bias Level 20/1000; Normal mode; DC-Couple; Pulse Duration 6 μs (internal control); Anticoincidence and Internal Strobe (rear-panel controls).

480 Pulser: Attenuated output.

459 5 kV Detector Bias Supply: Leave at zero until all other connections and adjustments have been made; consult the instructions for the HPGe detector to determine both the polarity and the amplitude of bias that are to be used, and apply the correct amount of bias in the correct polarity when ready to operate→ Make electronic interconnections fig 7.7

2. Place the ^{60}Co source from source kit SK-1G ~1 cm from the face of the detector. Adjust the gain of the 572 Amplifier so that the 1.33-MeV gamma has an amplitude of 6 V at the amplifier output. The two lines for 1.17 and 1.33 MeV should be quite easily seen on the oscilloscope. Check the output from the 444 Gated Biased Amplifier to make sure it looks reasonable.

3. Observe the display of the spectrum on the MCA. Adjust the bias level and gain on the 444 and the gain on the 572 until the two sharp photopeaks are positioned as shown in Fig. 7.8. In this measurement the two photopeaks should be separated by at least 200 channels, based on 1024 channels total.

4. From the positions of the two photopeaks make a calibration curve of energy (y direction) vs channel number (x direction) and determine the keV/channel.

EXERCISES

a. What is the resolution in keV for the two photopeaks? How does this compare in value with the detector's resolution specifications?

b. From the data, determine the energies of the Compton edges for the two gammas. How do these compare with the values that were calculated from the formula used in Experiment 3?

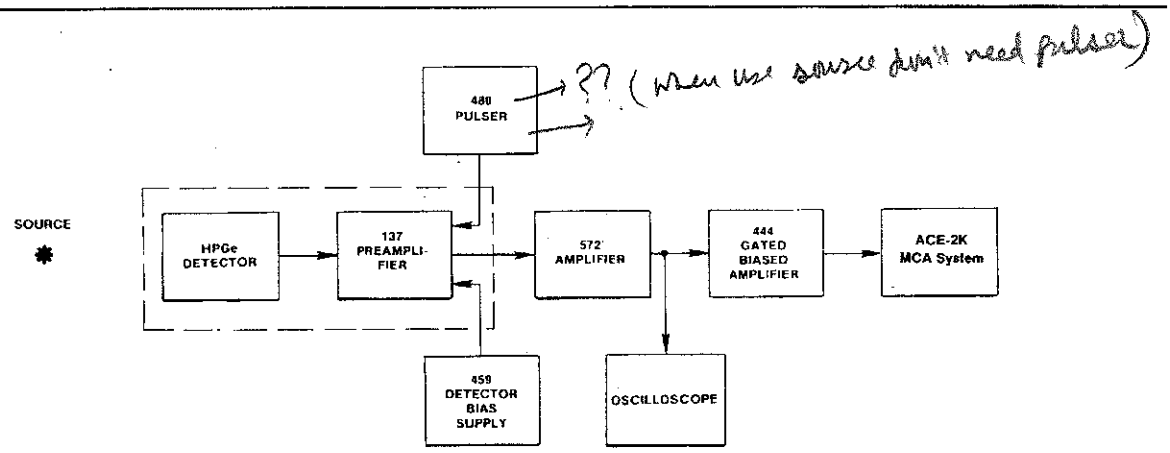

Fig. 7.7. Electronic Interconnections for Experiment 7.1.

5. Turn on the 480 Pulser and adjust the output so that the pulser peak falls about half-way between the 1.17- and 1.33-MeV peaks. After the pulser has produced enough counts for its peak channel to have 1000 counts, read that portion of the analyzer memory and determine the resolution of the pulser. This is the electronic resolution, R(E). The contribution from the detector to the overall resolution can be calculated from the formula

$$\text{system resolution} = \sqrt{[R(d)]^2 + [R(E)]^2} \qquad (1)$$

where R(d) is the detector resolution and R(E) is the electronic resolution. These resolutions are said to add in quadrature. There is a lower limit to R(d) which is energy-dependent. The recoil electron that is produced in the gamma interaction loses energy in the HPGe detector by dE/dx. The average energy required to produce an ionization in germanium is 2.95 eV/electron-hole pair. Thus for a 1.5-MeV recoil electron there would be 5.08 x 10^5 electron-hole pairs produced. The production of electron-hole pairs is a process that is statistical in nature, and hence there are fluctuations in the actual number produced. When the proper statistics are used, the theoretical lower limit to R(d) is given by

$$R(d) = K\sqrt{F \cdot E}\,, \qquad (2)$$

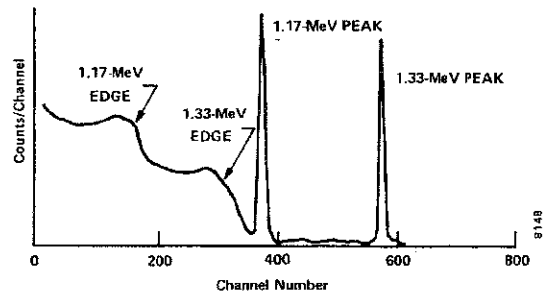

Fig. 7.8. Locating the Two Photopeaks for ^{60}Co in the HPGe Spectrum.

where K is a constant, E is the energy of the photon in MeV, and F is the statistical Fano factor. To a very good approximation this equation reduces to

$$R(d)\ (\text{in keV}) = 1.35\sqrt{E\ (\text{in MeV})}. \qquad (3)$$

Solving Eq. (3), the theoretical lower limit of detector resolution is 1.44 keV for a 1-MeV gamma and is 4.5 keV for a 10-MeV gamma.

EXERCISES

c. Calculate the values of R(d) from Eq. (3) for the values of E in Table 7.2.

Table 7.2

Energy (MeV)	Theoretical $R(d)$ (keV)
0.1	
0.3	
0.5	
1.0	
3.0	
6.0	
8.0	
10.0	

d. Make a plot of the values from Table 7.2 on linear graph paper. From Eq. (1) calculate the experimental R(d) for the 1.33-MeV peak of ^{60}Co. How does this compare with the theoretical limit? Remember that the R(d) theory is the absolute lower limit of the resolution value.

EXPERIMENT 7.2

Photopeak Efficiency for HPGe Detectors

Resolution with HPGe detectors is better by a factor of 30 or more than that obtained with NaI(Tl) conventional detectors. Coupled with this dramatic increase in resolution is a compromise of the photopeak efficiency. The pricing of HPGe detectors is related to their photopeak efficiency. The standard method for comparing the efficiencies of HPGe detectors with NaI(Tl) detectors is to compare their counting rates at the 1.33-MeV line of ^{60}Co, using a standard distance of 25 cm from the source to the detector face and placing the source on the detector axis.

The resolution of the HPGe detectors is so many times better than that of the NaI(Tl) that the ability to see a photopeak above the Compton distribution is considerably enhanced. Consider a simple example in which the efficiencies of the HPGe and NaI(Tl) are assumed to be the same. In a particular experiment we observe 10,000 counts under the photopeak for each detector. If the resolution of the HPGe detector is only 10 times that of the NaI(Tl) detector, the HPGe photopeak will have 10 times the maximum number of counts that the NaI(Tl) detector has, because the area under the photopeak (10,000 for this example) is approximately proportional to the width times the height of the peak. Since the width of the HPGe peak is only 1/10 the width of the NaI(Tl) peak, its height must be 10 times as great.

This example can easily be extrapolated to real situations where the advantages of superior resolution are very important. For example, Fig. 7.9 shows the striking differences for a spectrum obtained on a mixed sample of ^{76}As, ^{122}Sb, and ^{124}Sb with each of the two types of detectors. Each of the closely spaced energy lines is shown separately in the HPGe spectrum and are all included in a single broad photopeak in the NaI(Tl) spectrum.

In this experiment, we will measure some of these photopeak efficiencies and also determine the peak-to-Compton ratio for an HPGe detector.

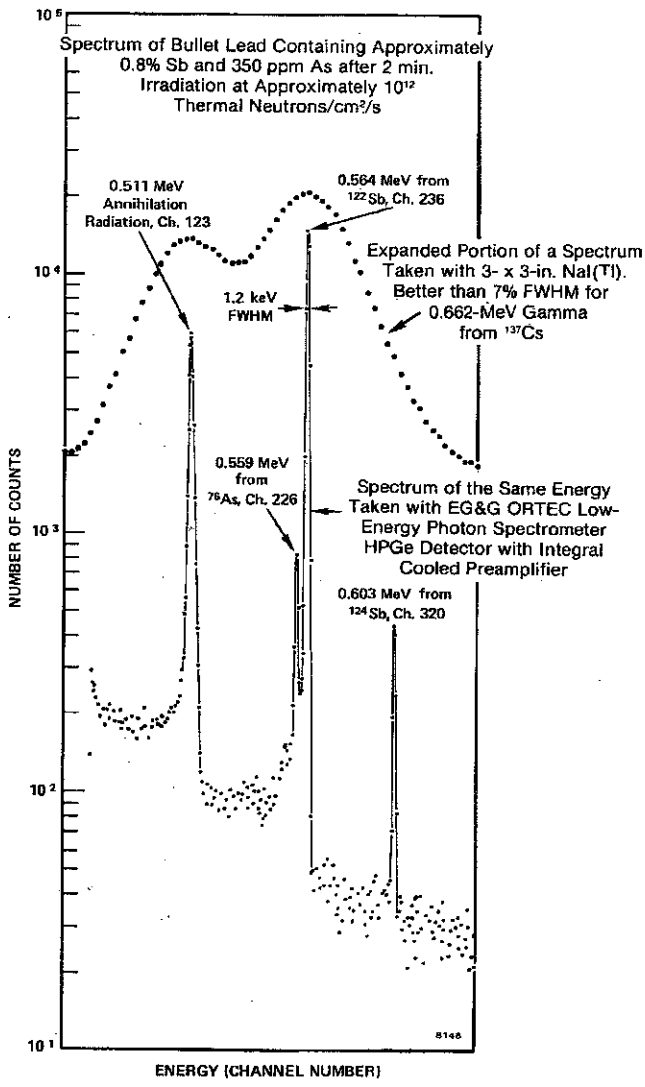

Fig. 7.9. Comparative Spectra Taken with HPGe and NaI(Tl) Detectors.

Procedure

1. Use the same equipment setup that was used for Experiment 7.1. Adjust the gain of the 572 and bias level and gain of the 444 for a ^{60}Co spectrum similar to that of Fig. 7.10.

2. Accumulate the spectrum in the MCA for a time period long enough to determine heights h_1 and h_2 to a fair degree of accuracy. In Fig. 7.10, h_1 is the 1.33-MeV photopeak and h_2 is the maximum for the comparable Compton distribution, normally located just below the Compton edge. Read the data from the analyzer.

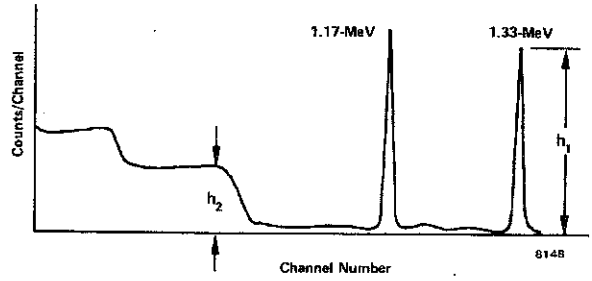

Fig. 7.10. Typical Distribution of ^{60}Co Spectrum for Experiment 7.2.

EXERCISE

a. Calculate the peak-to-Compton ratio, which is h_1 divided by h_2 in Fig. 7.10. Compare your value with the value for this ratio for the detector; check with your laboratory instructor for the record of the ratio.

3. Clear the spectrum from the MCA. Place a 10-μCi ^{60}Co source at a distance of exactly 25.0 cm from the face of the detector.

4. Accumulate a spectrum for this source for a time period long enough for the sum of counts under the 1.33-MeV photopeak to be about 3000. Read the data from the analyzer and be sure to record the live time for the measurement.

EXERCISES

b. Calculate the number of counts per second for the events that were recorded in the 1.33-MeV photopeak; call this R_1:

$$R_1 = \frac{\Sigma_{pp}}{\text{time in seconds}} . \qquad (4)$$

c. The rate, R_1, from Eq. (4) is to be compared with the rate, R_2, that is expected for the same source when it is located 25.0 cm from the face of a 3- x 3-in. NaI(Tl) detector. The efficiency of this size NaI(Tl) detector for a source-to-detector distance of 25.0 cm is given as 1.2×10^{-3}, which is from the "Gamma Ray Spectrum Catalog," by R. L. Heath, Idaho Falls Report IDO-16880. Using ϵ_1 for this number, the number of counts, (N), that you would observe under the photopeak for a 3- x 3-in. NaI(Tl) detector at 25.0 cm source distance is given by

$$N = \epsilon_1 A t , \qquad (5)$$

where A is the gamma activity of the source in counts per second and t is the live time in seconds. The rate R_2 will then be

$$R_2 = \frac{N}{t} = \epsilon_1 A . \qquad (6)$$

Since ^{60}Co has a 1.33-MeV gamma ray for each decay, A is given by

$$A = 3.7 \times 10^4 \ (x), \qquad (7)$$

where x is the source strength in microcuries (μCi).

Calculate R_2 from Eq. (6). The relative photopeak efficiency is obtained for the detector by

$$\text{relative photopeak efficiency} = \frac{R_1}{R_2} \times 100. \qquad (8)$$

Calculate this value for your measurement and compare it with the value that is recorded for the detector; check with your laboratory instructor for the record of the detector's efficiency.

EXPERIMENT 7.3

Escape Peaks and Efficiency for HPGe Detectors

As discussed earlier, when an incident gamma with sufficient energy enters the crystal it can create an electron-positron pair. When the positron annihilates, two gammas with equal energy at 0.511 MeV are produced and these leave with an angular separation of 180°. In Fig. 7.3 these two gammas are shown as γ_1 and γ_2. For small detectors it is very probable that both γ_1 and γ_2 will escape from the detector before they make any further interactions in the crystal. The energy thus absorbed would be $E_\gamma - 1.02$ MeV and is shown as the Double-Escape Peak in Fig. 7.4. As the detector size is increased, the probability is greater that either γ_1 or γ_2 will make a photoelectric interaction within the crystal. If one of these gammas does make a photoelectric interaction, the energy of the event that is recorded in the detector is the Single-Escape Peak in Fig. 7.4. For even larger detectors the probability of photoelectric interactions is further increased when both γ_1 and γ_2 interact and the total energy of the gamma is absorbed in the crystal. Figure 7.11 shows some measurements that have been made for coaxial and planar HPGe detectors. From this figure the ratios of Full-Energy, Double-Escape Peak, and Single-Escape Peak efficiencies can be determined by inspection for the size of detector that is identified in the figure.

To see how the measurements were made for Fig. 7.11, consider the E_γ of 2.511 MeV shown in Fig. 7.4. Assume that the

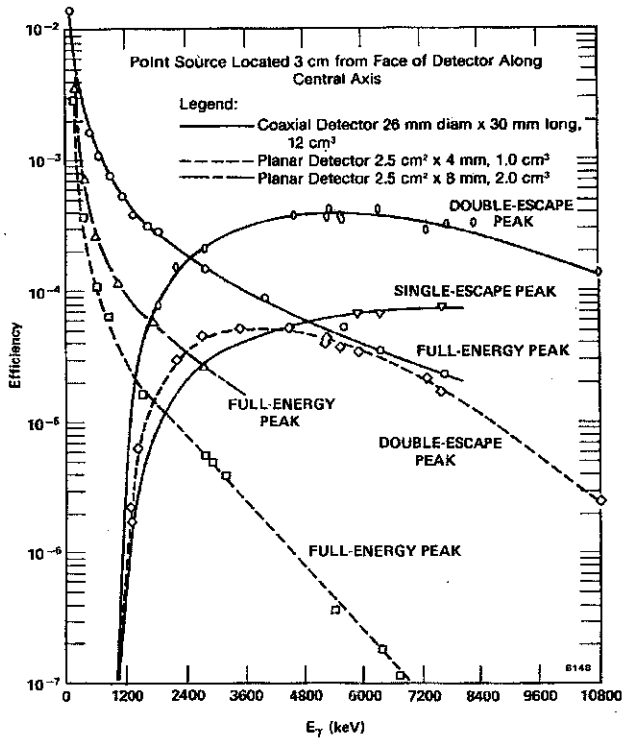

Fig. 7.11. Measured Efficiencies for HPGe Detector.

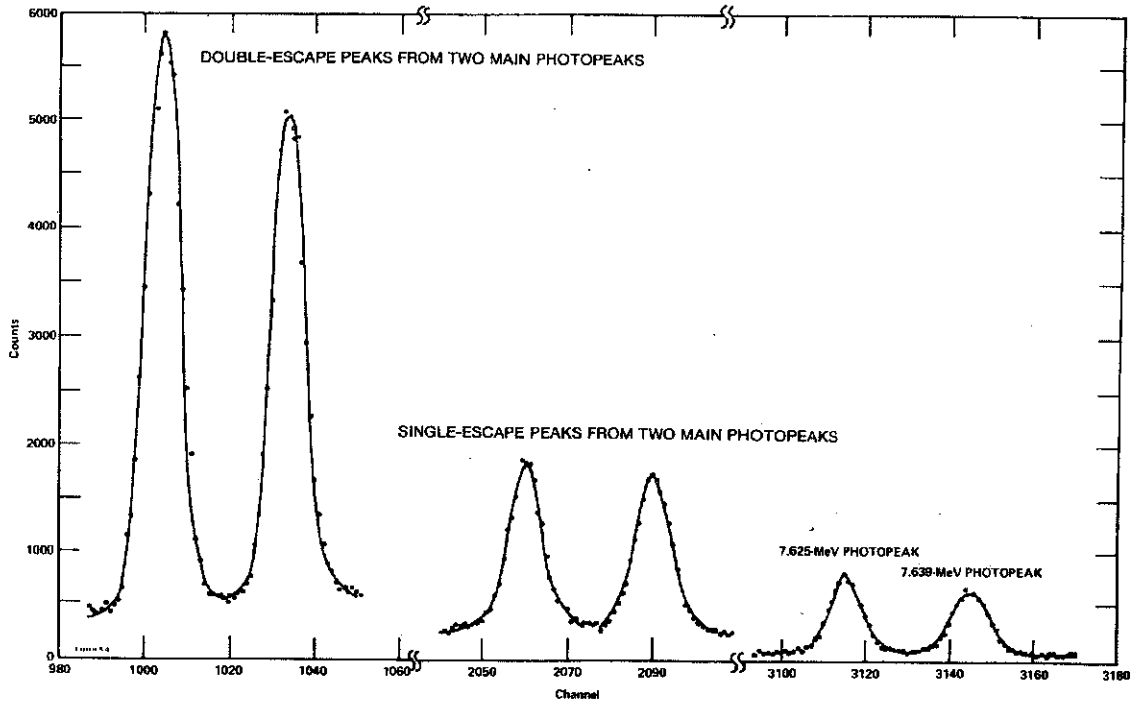

Fig. 7.12. Typical High-Energy Gamma Spectrum from a Neutron Source with Iron Scatterer.

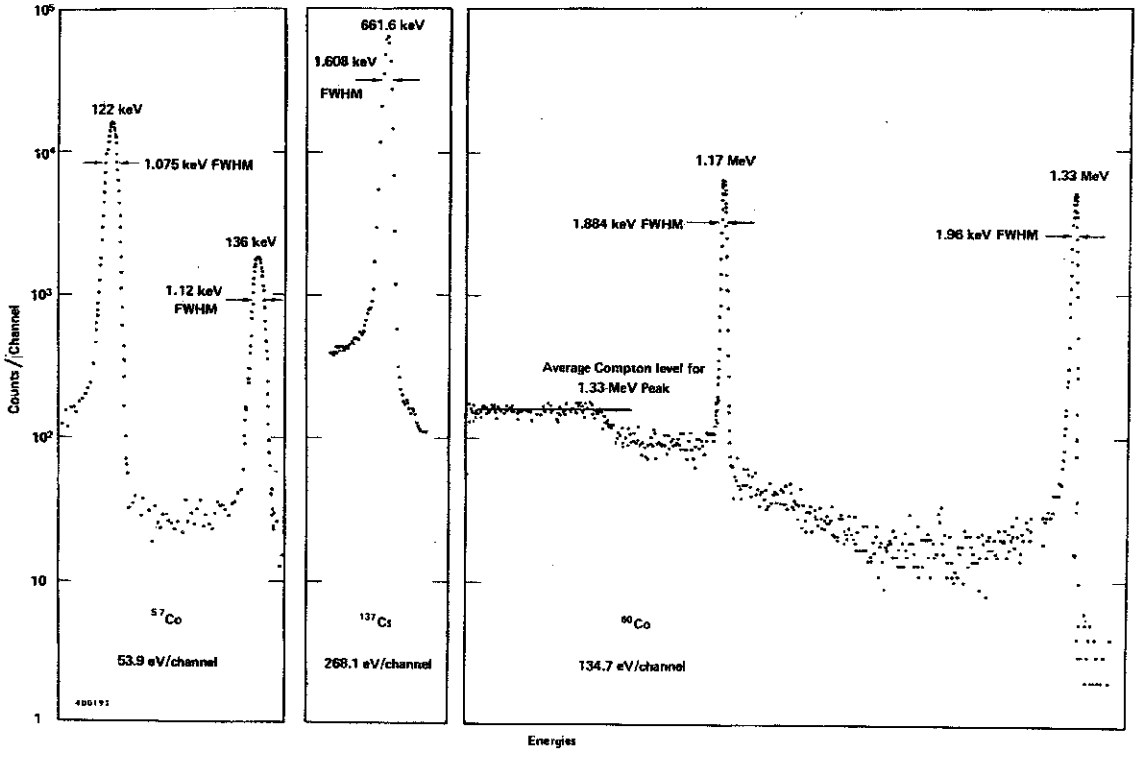

Fig. 7.13. Typical Spectral Response of an EG&G ORTEC HPGe Detector to Various Gamma-Ray Energies.

Compton distribution has been subtracted for each peak in Fig. 7.4 and that the following sums have been measured:

Σ at Full Energy, 2.511 MeV = 6000,
Σ at Single-Escape, 2.00 MeV = 1000,
Σ at Double-Escape, 1.489 MeV = 3000.

From these numbers the simple ratios can be obtained.

Procedure

1. Use the same equipment setup that was used for Experiment 7.1. Use the ^{60}Co and ^{137}Cs gamma sources from SK-1G. Adjust the system gain and bias on the 572 and 444 to calibrate the analyzer roughly from 1 to 3 MeV.

2. Remove the energy calibration sources and use a ^{228}Th (or other high-energy) source to accumulate a spectrum. Accumulate for a period of time long enough to see all the pronounced peaks in the spectrum. Read the data from the analyzer.

EXERCISES

a. Plot the spectrum on semilog graph paper. On the plot identify all the major peaks and the corresponding escape peaks. Compare the energies at these peaks with those that are identified with the source.

b. Calculate the escape-peak ratios. Define Σ_f as the sum of counts under the full-energy peak, Σ_1 as the sum under the single-escape peak, and Σ_2 as the sum under the double-escape peak. Be sure to subtract the Compton distribution from these sums. Then determine the ratios Σ_f/Σ_1, Σ_f/Σ_2, and Σ_2/Σ_1. How do these ratios compare with those the laboratory instructor has for the ^{228}Th source and the detector you are using?

EXPERIMENT 7.4
(Optional, recommended if Experiments 16, 17, or 18 are to be done)

The Response of HPGe Detectors to High-Energy Gammas

If an isotopic neutron source of the Am-Be type is available, it is possible to obtain high-energy gammas from this source. The neutrons from the source are produced by

$$^{9}Be + \alpha \rightarrow {}^{12}C + n, \qquad (9)$$

The Q value for the reaction is ~5 MeV. Since the alpha energies from most sources are also ~5 MeV, it is possible to produce neutrons with these sources up to 10 MeV. The neutron spectrum from these sources shows a distribution of neutron energies up to this maximum energy of ~10 MeV. What is of more importance is that in the reaction it is also possible for ^{12}C to be left in an excited state. The de-excitation of ^{12}C is by gamma emission. Gammas from the second excited state of ^{12}C have an energy of 7.656 MeV and make an excellent source of high-energy gammas.

Procedure

1. Use the same equipment setup that was used for Experiment 7.1. Use the ^{60}Co source and the pulse generator to adjust the gain and bias of the system so that the MCA range is ~3 to 8 MeV.

2. Use a block of paraffin ~6 in. thick between the detector and the neutron source, and place the source ~12 in. from the detector. The paraffin will thermalize the neutrons from the source without attenuating the high-energy gammas. In some cases the neutron source is in a paraffin howitzer; if this is the case, place the source close to the outside of the howitzer.

3. Accumulate a spectrum. This will require several hours, and sometimes overnight runs are necessary. Read the data from the analyzer.

EXERCISE

Plot the spectrum on semilog paper and identify all the peaks. As in Experiment 7.3, calculate the ratios Σ_f/Σ_1, Σ_f/Σ_2, and Σ_2/Σ_1.

For your reference, Fig. 7.12 is a plot on linear graph paper for a typical neutron source with an iron scatterer. The reaction is ^{56}Fe(n,γ)^{57}Fe, which yields two high-energy gammas from the ^{56}Fe scatterer. The main photopeak energies are 7.639 and 7.625 MeV.

The resolution of a gamma line is dependent on the gamma energy of the peak. The student can easily verify this by measuring the resolution of the detector for the sources available in the laboratory. Figure 7.13 shows the spectral response and resolution of several common sources for an HPGe detector.

References

1. A. Coche and P. Siffert, *Lithium Drifted Silicon and Germanium Detectors in Semiconductor Detectors*, G. Bertolini and A. Coche Eds., Elsevier-North Holland, Amsterdam (1968).

2. J. C. Phillppot, *IEEE Trans. Nucl. Sci.* **NS-17**(3), 446 (1970).

3. F. Adams and R. Dams, *Applied Gamma Ray Spectrometry*, 2nd Edition, Pergammon Press, Ltd. (1970).

4. U. E. P. Berg, H. Wolf, *et al., Nucl. Instrum. Methods* **129**, 155 (1975).

5. C. Meixner, *Nucl. Instrum. Methods* **119**, 521 (1974).

6. D. M. Walker and J. M. Palms, *IEEE Trans. Nucl. Sci.* **NS-17**(3), 296 (1970).

7. M. L. Stelts and J. C. Browne, *Nucl. Instrum. Methods* **133**, 35 (1976).

8. 20th Nuclear Science Symposium, *IEEE Trans. Nucl. Sci.* **NS-21**(1) (1974).

9. 19th Nuclear Science Symposium, *IEEE Trans. Nucl. Sci.* **NS-20**(1) (1973).

10. C. M. Lederer and V. S. Shirley, Eds., Table of Isotopes, 7th Edition, John Wiley and Sons, Inc., New York (1978).

11. G. F. Knoll, *Radiation Detection and Measurement*, Wiley, New York (1979).

12. Nuclear Data Sheets, Edited by the Nuclear Data Project, Academic Press, New York and London.